Planta (2023) 258:109
https://doi.org/10.1007/s00425-023-04263-4

ORIGINAL ARTICLE

Salinity alleviates arsenic stress-induced oxidative damage via antioxidative defense and metabolic adjustment in the root of the halophyte *Salvadora persica*

Monika Patel[1,2] · **Asish Kumar Parida**[1,2]

Received: 30 August 2023 / Accepted: 8 October 2023 / Published online: 1 November 2023

Abstract

Main conclusion **Arsenic tolerance in the halophyte *Salvadora persica* is achieved by enhancing antioxidative defense and modulations of various groups of metabolites like amino acids, organic acids, sugars, sugar alcohols, and phytohormones.**

Abstract *Salvadora persica* is a facultative halophyte that thrives under high saline and arid regions of the world. In present study, we examine root metabolic responses of *S. persica* exposed to individual effects of high salinity (750 mM NaCl), arsenic (600 µM As), and combined treatment of salinity and arsenic (250 mM NaCl + 600 µM As) to decipher its As and salinity resistance mechanism. Our results demonstrated that NaCl supplementation reduced the levels of reactive oxygen species (ROS) under As stress. The increased activities of antioxidant enzymes like superoxide dismutase (SOD), catalase (CAT), glutathione peroxidase (GPX), and glutathione reductase (GR) maintained appropriate levels of ROS [superoxide ($O_2^{\bullet-}$) and hydrogen peroxide (H_2O_2)] under salinity and/or As stress. The metabolites like sugars, amino acids, polyphenols, and organic acids exhibited higher accumulations when salt was supplied with As. Furthermore, comparatively higher accumulations of glycine, glutamate, and cystine under combined stress of salt and As may indicate its role in glutathione and phytochelatins (PCs) synthesis in root. The levels of phytohormones such as salicylate, jasmonate, abscisic acid, and auxins were significantly increased under high As with and without salinity stress. The amino acid metabolism, glutathione metabolism, carbohydrate metabolism, tricarboxylic acid cycle (TCA cycle), phenylpropanoid biosynthesis, and phenylalanine metabolism are the most significantly altered metabolic pathways in response to NaCl and/or As stress. Our study decoded the important metabolites and metabolic pathways involved in As and/or salinity tolerance in root of the halophyte *S. persica* providing clues for development of salinity and As resistance crops.

Keywords Arsenic stress · Metabolites · Phytochelatins · Salinity · *Salvadora persica* · TCA cycle

Abbreviations

APX	Ascorbate peroxidase
CAT	Catalase
GPX	Glutathione peroxidase
GR	Glutathione reductase
GSH	Reduced glutathione
GSSG	Oxidized glutathione
IBA	Indole-3-butyric acid
JA	Jasmonic acid
SA	Salicylic acid
SOD	Superoxide dismutase
TCA cycle	Tricarboxylic acid cycle

Communicated by Dorothea Bartels.

✉ Asish Kumar Parida
asishparida@csmcri.res.in

[1] Plant Omics Division, CSIR- Central Salt and Marine Chemicals Research Institute (CSIR-CSMCRI), Gijubhai Badheka Marg, Bhavnagar 364002, Gujarat, India

[2] Academy of Scientific and Innovative Research (AcSIR), Gaziabad 201002, India

Introduction

Heavy metals (HMs) and metalloid contamination emerged as global environmental concerns due to the increasing industrial and agricultural development. HMs naturally occur in soil at low concentrations, but they are potent soil

contaminants due to their wide distribution. Undoubtedly, a few heavy metals (like Zn, Cu, and Ni) are crucial for the plant growth. However, most are toxic and may threaten the regular metabolic activity of the plants even at low concentrations. The contamination of heavy metal (loid)s at the interfaces of soil–food crop has become a severe threat to food security, human health, and sustainable agricultural productivity (Rai et al. 2023). The plants uptake excess trace metals from the soil that exert toxicity. Heavy metal (loid)s content in the rhizosphere modulates plants' normal physiological and metabolic functioning. The plants absorb HM through the root system by both active and passive transport to the above-ground tissue via the xylem, which affects various physiological and biochemical mechanisms. Moreover, increased toxic metal ions in the soil compete with other vital nutrients for absorption and cause nutrient scarcity in plants (Nikalje and Suprasanna 2018). Among various contaminants, arsenic (As) is an extremely toxic metalloid for the plants. Arsenic (As) is regarded as a redox metalloid, class 1 carcinogen, mutagen, and teratogen imparting the entire biosphere (Sarath et al. 2022). It is a ubiquitous element, usually found in minute amounts in soil, rock, water, and air. Arsenic is a highly mobile metalloid that can efficiently translocate from root to harvestable parts of the plants. Arsenic was absorbed by the plants through the roots via same channels that are used for the mineral nutrients absorption (Martínez-Castillo et al. 2022). The toxicity of As inhibits the plant growth and biomass, reduces photosynthesis and chlorophyll degradation, impairs minerals and nutrients, affects water status, creates oxidative stress, alters hormonal content, and eventually causes plant death (Vromman et al. 2018). Similarly, soil salinity has also been recognized as a severe threat to agriculture and food production on a global scale. With increasing population growth and rapid economic development, the coastal areas of many countries are contaminated by heavy metals (loids). A transition area of ocean and land, coastal regions, and sediments typically suffer from the concurrent contamination of excess salinity and heavy metals. Moreover, contamination of toxic metalloids in saline soil is difficult to remediate because salinity increases the mobility of metals in soil (Liu et al. 2019). Salinity hinders various physiological and biochemical processes in plants and causes ion toxicity and osmotic stress, which disturb redox homeostasis and subsequently accelerate ROS production. Ultimately, excessive ROS causes oxidative injury to the plant tissues.

The plants execute intricate defense mechanisms to survive and safeguard themselves from the toxic effects of heavy metals. The practical approaches include compartmentalization and sequestration in organelles, inactivation of heavy metals by complex formation with organic ligands, and elimination using ion channels, transporters, and signaling molecules (Jamla et al. 2021). Most of the plants retain toxic substances in their roots. Roots are the initial contacting tissue of plants with metal toxicity in the environment. Roots restrict the metal uptake by changing the rhizosphere pH and by secretion of some exudates like organic acids and amino acids, thus acting as the first line of defense. The heavy metals reduce root diameter, elongation, and root hair growth (Rahman et al. 2021). The most crucial mechanisms in roots to overcome the heavy metal stress include metal ion exclusion or avoidance, excretion or hyperaccumulation and complexation of heavy metal with thiol compounds within the root cells and vacuolar sequestration, thereby avoiding their interaction with sensitive components of the cell (Patel and Parida 2021). Several plants do not possess specific features like metal exclusion and excretion to eliminate excess heavy metals. In this case, the root absorbs metallic ions resulting in synthesis or deposition of organic osmolytes for chelation, intracellular complexation, and compartmentalization of metal (loid)s in the cytosol. Different chelators highly control the translocation of metallic ions from the root to the xylem. The peptides, organic acids, and amino acids are the potential ligands for specific metal bindings, translocation, and storage within the plant.

Other metabolites like sugars and phytohormones play essential roles in long-distance signaling. The polyphenols tend to chelate metallic ions and reduce lipid peroxidation by trapping the lipid alkoxyl radical. The "omics"-based tool, metabolomics, reveals the relation between the plants and environment, which is accomplished by detailed understanding of metabolic regulation, metabolic pathways, phenotype, and plant growth (Zhang et al. 2016; Rahman et al. 2022). Identification and quantification of the endogenous metabolites provide information on the key compounds and disclose some novel pathways playing important roles in plant stress tolerance.

The remediation of heavy metal pollution in saline soil is a challenging task. The soil desalinization is critical to control the toxicity of heavy metals in coastal lands. Although a majority of crop plants are salt sensitive, a group of plants called "halophytes" can grow in high-saline areas. To adapt under environmental stress conditions, the halophytes activate a variety of stress-related genes and metabolites (Patel and Parida 2022; Patel et al. 2022). Halophytes reduce soil salinity and remediate metal toxicity, thus playing a dual function in soil reclamation. Heavy metal (loid)s-resistant halophytic plant species could be crucial for the restoration of heavy metal-affected saline and non-saline soil. *Salvadora persica* L. (a facultative halophyte) flourish in semi-arid, arid, and coastal lines of western India to the Middle East (Phulwaria et al. 2011). *S. persica* is adapted to tolerate high salt and water stress environments. In addition, it is widely adapted to dry to marshy coastal land, dunes to heavy soil, and non-saline to extremely saline areas (Reddy et al. 2008). This halophyte has been studied for its salinity and

drought tolerance mechanism at physiological, biochemical, and metabolomics levels for the identification of stress tolerance markers that can be used for the development of salt- and drought-tolerant crops and their potential use for land reclamation (Rangani et al. 2016, 2020; Kumari and Parida 2018). In our preceding study, *S. persica* has been identified as arsenic hyperaccumulating halophyte for phytoremediation of As-contaminated saline and non-saline soil (Patel and Parida 2021). *S. persica* accumulates higher As and phytochelatin (PCs) in root than in shoot tissue under combined stress of As and salinity (Patel and Parida 2021). In addition, exogenous salinity reduced the uptake of As in shoot (70%) and root (58%) under high As conditions and allows better biomass production. Our results demonstrated that most of the As are chelated by PCs and other metabolites and safely stored in the root vacuoles. This ultimately limits the entry of As in the above-ground tissue to protect the photosynthetic machinery, thereby enhancing As tolerance of *S. persica*. To the best of our knowledge, root-specific metabolomic study under salinity and/or As stress conditions has not been reported earlier in *S. persica*. Therefore, in the present investigation, we report ROS scavenging attributes and metabolic alteration to identify potential metabolites and metabolic networks that can be targeted to improve As and salinity resistance in crop plants.

Materials and methods

Plant material, salinity and arsenic treatments, and sample collection

Seeds of *S. persica* were picked from CSMCRI (salt farm area), Bhavnagar, India, and shade-dried completely. Seed disinfection, germination, and seedling irrigation were done as reported earlier by Rangani et al. (2018). Two-month-old seedlings were acclimatized in standard hydroponic conditions (14 h per day photoperiod using white light with temperature of 25 ± 2 °C) for 2 weeks. After 2 weeks of acclimatization, various concentrations of salt and/or arsenic treatments were given: 750 mM NaCl, 600 µM As and 600 µM As + 250 mM NaCl. The arsenic and salt stress were applied in the form of NaCl and $Na_2HAsO_4{\cdot}7H_2O$. The control seedlings were grown in regular Hoagland's medium devoid of As and NaCl. After 14 d of treatments, the root samples were collected for evaluation of different parameters as discussed below.

Oxidative stress biomarkers

For assessment of lipid peroxidation (MDA), the root samples were extracted in 0.1% tricarboxylic acid (TCA), centrifuged (at 12,000 g for 15 min), and the supernatant was collected. Then 2 ml of 0.5% thiobarbituric acid (TBA) prepared in 20% TCA was mixed with 500 µl of supernatant and boiled at 95°C for half an hour. After cooling down the reaction mixture, the optical density was measured at 532 and 600 nm. The concentration of MDA was calculated from the extinction coefficient of 155 mM^{-1} cm^{-1}.

The concentration of superoxide radical ($O_2^{\bullet-}$) was determined as reported by Yang et al. (2011). In brief, root tissue was homogenized in 2 ml of phosphate buffer (pH 7.8) and 5% (w/v) polyvinylpolypyrrolidone (PVPP). After centrifugation at 10, 000 g for 10 min at 4 °C, 0.5 ml of the supernatant was mixed with reaction mixture containing 50 mM phosphate buffer (pH 7.8) and 10 mM hydroxylamine hydrochloride and kept for 30 min at room temperature. Then 0.5 ml of 17 mM sulfanilamide and 0.5 ml of 7 mM α-napthylamide were added to the reaction mixture and again incubated for 30 min at room temperature. The optical density was taken at 530 nm. The concentration of $O_2^{\bullet-}$ was calculated by the standard curve prepared against $NaNO_2$ (0–50 µg ml^{-1}).

The H_2O_2 content in the root was determined following the procedure of Ibáñez et al. (2010). The fresh root tissue was homogenized in 1 M perchloric acid in the presence of 5% PVPP. After centrifugation (at 15, 000 g for 15 min at 4 °C), the supernatant was neutralized with 5 M K_2CO_3 in the presence of 0.3 M phosphate buffer (pH 5.6). The reaction mixture was spin to pull out the excess $KClO_4$ and the supernatant was collected. Then 0.2 ml of the supernatant was mixed with 0.8 ml of FOX-1 reagent (100 µM $FeNH_4SO_4$, 25 mM H_2SO_4, 250 µM xylenol orange, and 100 mM sorbitol). The reaction mixture was kept in dark condition for 30 min and then the absorbance was measured at 560 nm. H_2O_2 content was calculated from the standard curve prepared against H_2O_2 (0–20 µmol).

Analysis of antioxidant enzymes

The root tissue was crushed in liquid N_2 and homogenized in pre-chilled potassium phosphate buffer [pH 7.0, 1 mM EDTA, and 5% (w/v) polyvinylpolypyrrolidone (PVPP)]. The content was spin at 15,000 g for 10 min at 4 °C. The supernatant of the root extract was used for the determination of activity of the antioxidant enzymes. The total protein concentration was determined as reported by Bradford (1976).

Superoxide dismutase

Superoxide dismutase (SOD) activity was assayed in terms of photoinhibition of nitro blue tetrazolium (NBT) by the enzyme extract employing the method explained by Rangani et al. (2016). The reaction cocktail containing 50 mM KPO_4 (pH 7.8), 58 µM NBT, 9.9 mM L-methionine, 2.4 µM

riboflavin, 0.025% Triton X-100 was used for the assay of SOD and the absorbance was recorded at 560 nm.

Catalase

Catalase (CAT) activity was assayed by recording the absorbance at 240 nm using a reaction mixture containing 10.5 mM H_2O_2 in KPO_4 (50 mM, pH 7.0) and extinction coefficient (ε) of 43.6 M^{-1} cm^{-1}.

Ascorbate peroxidase

Ascorbate peroxidase (APX) activity was measured as described earlier by Rangani et al. (2016). The reaction mixture contained 50 mM potassium phosphate (pH 7.0), 0.5 mM ascorbic acid, and 0.1 mM H_2O_2. The decrease in absorbance at 290 nm for 1 min was recorded, and the amount of ascorbate oxidized was calculated from ε of 2.8 mM^{-1} cm^{-1}.

Guaiacol peroxidase

Guaiacol peroxidase (POX) activity was measured following the protocol of Rangani et al. (2016). The reaction mixture consisted of 50 mM potassium phosphate (pH 7.0), 9 mM guaiacol, 19 mM H_2O_2, and 25 µl of enzyme extract. The formation of tetra guaiacol was measured at 470 nm and calculated by ε of 26.6 mM^{-1} cm^{-1}.

Glutathione reductase

Glutathione reductase (GR) activity was assayed following the protocol of Rangani et al. (2016) by recording the absorbance at 412 nm (ε = 14.15 mM^{-1} cm^{-1}) using the reaction mixture composed of 100 mM KPO_4 (pH 7.5), 0.75 mM DTNB, 1 mM EDTA, 1 mM oxidized glutathione (GSSG), and 0.1 mM NADPH.

Analysis of glutathione levels

The level of GSH (reduced glutathione) and GSSG (oxidized glutathione) was estimated according to the method of Parida and Jha (2010). The root tissue was homogenized in 5% sulfosalicylic acid. The content was centrifuged at 15,000 g for 15 min at 4 °C. Then the supernatant was neutralized by adding 7.5 M triethanolamine to pH 7.0. The neutralized aliquot (150 µl) was used for the estimation of total glutathione (GSSG + GSH). For GSSG analysis, the sample was pretreated with 2-vinyl pyridine for 1 h at 20 °C to mask the activity of GSH. From both types of samples, 50 µl aliquot was taken and mixed with 0.7 ml of 0.3 mM NADPH, 0.1 ml of 6 mM 5,5′- dithiobis-2-nitrobenzoic acid (DTNB), and 150 µl of 100 mM $KHPO_4$, 1 mM EDTA buffer (pH 7.5). Then 10 µl of glutathione reductase (50 U ml^{-1}) was added. The absorbance was read at 412 nm. The level of total glutathione, reduced GSH (total GSH – oxidized GSSG), and GSSG, was calculated using a standard curve prepared against GSH and GSSG.

Metabolite profiling using gas chromatograph–mass spectroscopy (GC–MS)

The extraction and derivatization of total root metabolites were performed as reported by Roessner et al. (2003). The root sample was extracted in methanol and chloroform (1:1, v/v) with the addition of 100 µl of ribitol (1 mg ml^{-1} solution) as an internal standard. The sample was sonicated for 5 min and then incubated at 70 °C for 15 min. After centrifugation (at 22,000 g for 15 min), the aqueous layer was vacuum dried. The vacuum-dried sample was derivatized in methoxyl amine hydrochloride prepared in pyridine and incubated for 120 min at 37 °C. For complete derivatization, N,O-bis(trimethylsilyl)trifluoroacetamide (BSTFA) was added and again incubated for 30 min at 37 °C. GC–MS analysis was performed using 2 µl of final sample volume in a GC–MS system (GC–MS-QP2010, Shimadzu, Kyoto, Japan). Helium was used as a carrier gas with adjusted flow rate of 1 ml per min. The inlet temp and ion source temperature were set at 300 °C and 250 °C, respectively. The mass spectra were recorded and the putative metabolites were identified by matching spectra in the NIST library. The metabolites were quantified by calculating the relative response ratio of the peak area of individual metabolites to that of internal standard ribitol, then finally normalizing it to the dry weight of the tissue and express in µg/g DW.

Amino acid profiling

The amino acids were analyzed using HPLC as per the method reported by Kwanyuen and Burton (2010). Amino acid separation and detection were performed using a HPLC system (Waters Alliance model, 2996-photodiode array detector) employed with Luna C18 reversed-phase column (Phenomenex, Torrance, CA, USA). For sample elution, mobile phase A (0.05% TEA, 0.15 M sodium acetate, and 6% CH_3CN, pH 6.4) and mobile phase B (H_2O: CH_3CN 4:6, v/v) were used at 1 ml per min flow rate following the linear mixing of mobile phase A and B. The amino acid spectra were observed at 254 nm, and the identification and quantification of individual amino acids were carried out from the spectra of amino acid standard mixture (AAS18, Sigma).

Phytohormonal profiling

The profiling of phytohormones was performed as per the protocol reported by Pan et al. (2010). The root samples

were homogenized with liquid N_2 and extracted with a mixture of isopropyl alcohol: H_2O: conc. hydrochloric acid (HCl) (2:1:0.002, by vol.). Then 1000 µl of dichloromethane (DCM) was added and mixed for half an hour at 4°C. After centrifugation for 5 min at 13,000 g, the lower phase was vacuum dried and finally dissolved in 100 µl methanol. The chromatographic separation was done using the HPLC system (Shimadzu) equipped with a photodiode array detector and autosampler (SIL-20ACHP). The elution of phytohormones was done using the Luna-C18 reverse-phase column with a mobile phase containing water and CH_3OH in the ratio of 7:3 v/v with 0.1% acetic acid with 1 ml/min flow rate. The quantification of different phytohormones was carried out by preparing the standard curves using individual standard hormones such as abscisic acid (ABA), salicylic acid (SA), jasmonic acid (JA), 3-indoleacetic acid (IAA), indole-3-butyric acid (IBA), zeatin, and gibberellic acid (GA_3) and expressed in µg/g DW.

Profiling of polyphenols

For the analysis of polyphenols, the root samples were homogenized in liquid N_2 and extracted in CH_3OH. After centrifugation (at 10,000 g for 5 min), the supernatant was collected, the pellet was washed thrice in methanol, and the supernatant was collected. The collected supernatant was dried in a vacuum concentrator and finally dissolved in the mixture of acetonitrile and dimethyl sulfoxide (DMSO) in a ratio of 1:1. The profiling of polyphenols was carried out by following the protocol of Kumar et al. (2008). The separation was carried out using mobile phase A (0.1% trifluoroacetic acid in H_2O) and B (0.1% trifluoroacetic acid in C_2H_3N) with a flow rate of 700 µl/min and at 27 °C. The polyphenols were simultaneously monitored at 254, 280, 320, and 370 nm. The identification of phenolic compounds was done based on the retention time of standard polyphenols and quantified by calibration curve of individual standard polyphenols such as gallic acid, chlorogenic acid, catechin, gentisic acid, quercetin, coumarin, cinnamic acid, apigenin, naringenin, and kaempferol.

Data processing and statistical analysis

The data were expressed as mean ± SD with minimum of five replicates ($n = 5$) from individual treatments used for all the analysis. The significant difference in metabolite levels among different groups was tested via student *t* test ($^*P < 0.1$, $^{**}P < 0.05$ and $^{**}P < 0.01$). Metaboanalyst 5.0 was used for principal component analysis (PCA), partial least squares-discriminant analysis (PLS-DA), heatmap, correlation, and pathway enrichment analysis. Sigma Plot v12.0 statistical software (Systat Software Inc., Chicago, IL, USA) was used for one-way analysis of variance (ANOVA) and Duncan's multiple range test ($P \leq 0.05$) for testing significant differences in ROS, antioxidative enzymes, and antioxidants.

Results

Supplementation of NaCl reduced the As-induced oxidative stress in the root

In *S. persica*, high salinity and As stress induced the accumulation of ROS in root tissue. The level of malonaldehyde (MDA) (+56.8, 47.3%), H_2O_2 (+31.5, 71.9%), and $O_2^{\bullet-}$ (+98.9, 183.5%) was significantly increased under high salinity and As, respectively (Fig. 1A–C). However, addition of NaCl with As significantly reduced H_2O_2 (−26.5%) and $O_2^{\bullet-}$ (−30.8%) content in comparison to solitary As (Fig. 1A–C). Hence, the low levels of salt help to reduce ROS toxicity in *S. persica*.

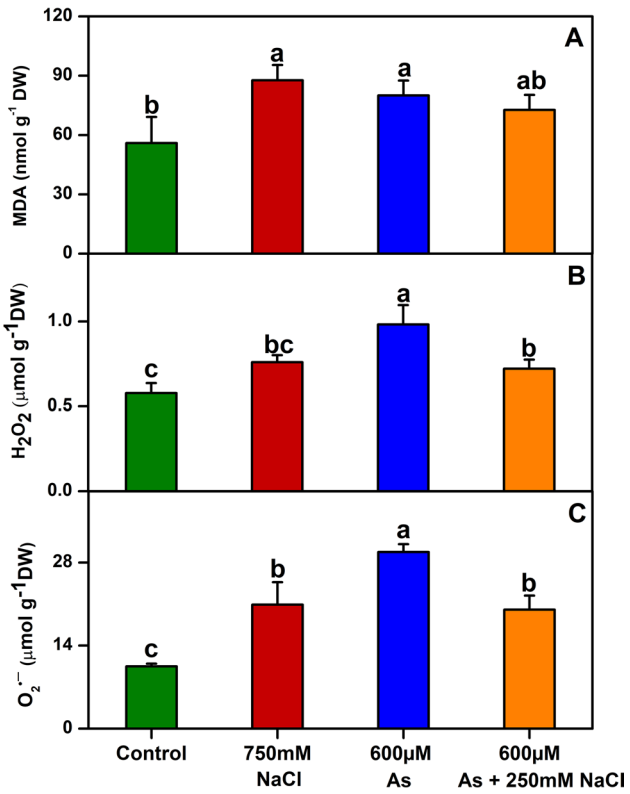

Fig. 1 Impact of NaCl and As on the accumulation of oxidative stress markers in the root of *S. persica*. **A** Lipid peroxidation measured in terms of MDA level. **B** H_2O_2. **C** $O_2^{\bullet-}$. The values are mean ± SD ($n = 5$). The different letters on the top of the error bars indicate statistically different means at $P \leq 0.05$ as analyzed by ANOVA and Duncan's multiple range test

Modulation in antioxidant enzymes under salinity and arsenic stress

The activities of antioxidative enzymes were differentially impacted by salinity and arsenic treatments in *S. persica*. The SOD activity was remarkably elevated in the root tissue under high NaCl (+ 1.83-fold) and As (+ 1.48-fold) stress compared to control. (Fig. 2A). However, it significantly downregulated (− 1.26-fold) by the addition of salt. CAT activity was significantly upregulated (+ 2.2-fold) under high As treatment. However, addition of low salt significantly reduced (− 1.41-fold) CAT activity under high As stress (Fig. 2B). The root APX activity showed a remarkable reduction (− 2.6-fold) under high As and/or salinity (Fig. 2C). GR activity was significantly upregulated under all stress treatments as compared to the control (Fig. 2D).

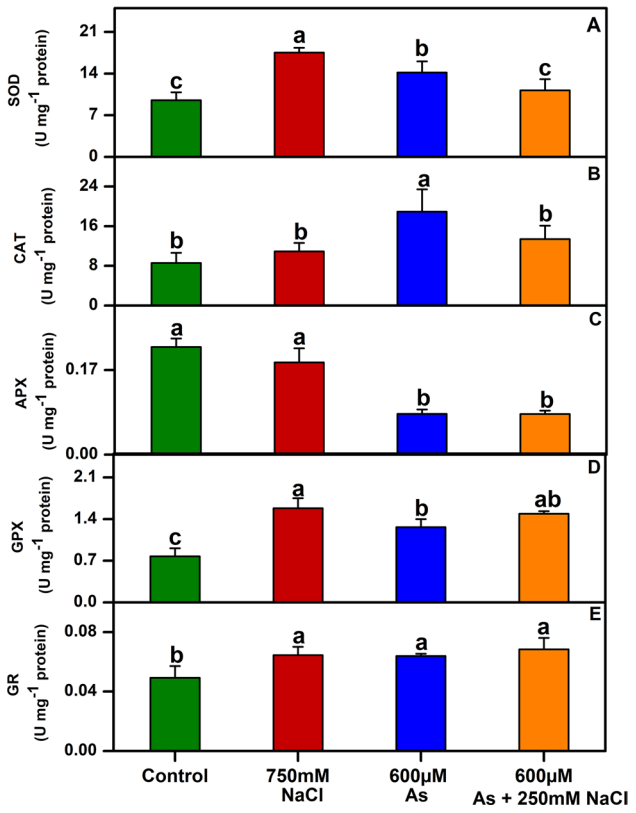

Fig. 2 NaCl and As-induced alterations in the activity of various antioxidative enzymes in the root of *S. persica.* **A** Superoxide dismutase (SOD). **B** Catalase (CAT). **C** Ascorbate peroxidase (APX). **D** Glutathione peroxidase (GPX). **E** Glutathione reductase (GR). The values are mean ± SD ($n = 5$). The different letters on the top of the error bars indicate statistically different means at $P \leq 0.05$ as analyzed by ANOVA and Duncan's multiple range test

Impact of NaCl and As on glutathione content in *S. persica* root

Glutathione is an important non-enzymatic thiol molecule, which is not only involved in ROS detoxification but it also plays an important role in the synthesis of phytochelatins (PCs) to chelate arsenic. The total glutathione content was significantly increased by high salinity and remained at par to the control level under high As with and without salinity stress (Fig. 3A). The level of GSH was significantly increased under high salinity (+ 142.5%), high As (+ 95.7%), and under combined stress (+ 137%) as compared to control (Fig. 3B). However, the GSSG content declined under high As (− 44.7%) and under As with salinity stress (− 51.3%) in comparison to control (Fig. 3C). The GSH/GSSG ratio remained high under As and/or salinity stress in the root (Fig. 3D). The results indicate the role of glutathione in ROS detoxification as well as PCs synthesis.

Salinity and/or As stress induced metabolic alterations in the root of *S. persica*

Metabolomics is an important approach to examine the functions of various metabolites intricate in physiological responses of the plants under abiotic constraints. The metabolites, the end products of cellular functions, regulate the phenotype of an organism under a stress condition by modulation of their synthesis and relative concentrations. Plant metabolomics deals with the diverse metabolic components categorized as amino acids, organic acids, polyphenols, phytohormones, and sugars, having diverse biological functions such as osmoregulation, stress signaling, ROS detoxification, membrane stabilization of cellular organelles, energy metabolism, and heavy metal chelation.

The root metabolome study of *S. persica* showed that a total of 53 metabolic compounds were identified in response to both NaCl and combined stress of As + NaCl, whereas 55 metabolites were identified in response to solitary treatment of As. The identified metabolites mainly include sugars, amino acids, phytohormones, polyphenols, and organic acids. PCA analysis was performed to exemplify the complex dataset and to identify and visualize sample grouping. The PCA plot indicates that control plants are differentiated from the stress-treated plants at the metabolite level and explaining 67.3% of the total variations (Fig. 4A). The metabolites such as aspartic acid, threonine, tyrosine, isoleucine, GA_3, tagatose, IAA, and sucrose were mainly contributed to PC 1. At the same time, the major contributors of PC 2 were aspartate, glutamic acid, serine, histidine, methionine, cystine, proline, SA, and JA (Fig. 4B). A total of 17 metabolites having variable importance in projection (VIP) score > 1 were considered as the most significant metabolites that may

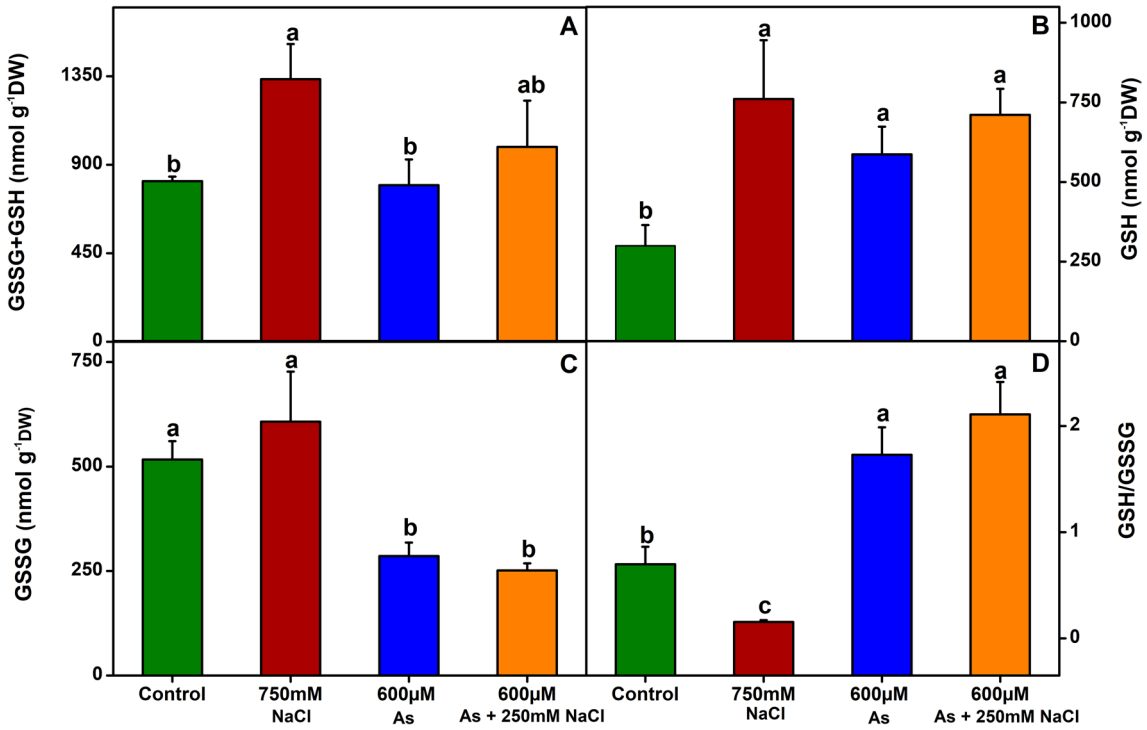

Fig. 3 Impact of NaCl and arsenic on glutathione content in the root of *S. persica*. **A** Total glutathione (GSSG + GSH). **B** Reduced glutathione (GSH). **C** Oxidized glutathione (GSSG). **D** GSH/GSSG ratio. The values are mean ± SD ($n = 5$). The different letters on the top of the error bars indicate statistically different means at $P \leq 0.05$ as analyzed by ANOVA and Duncan's multiple range test

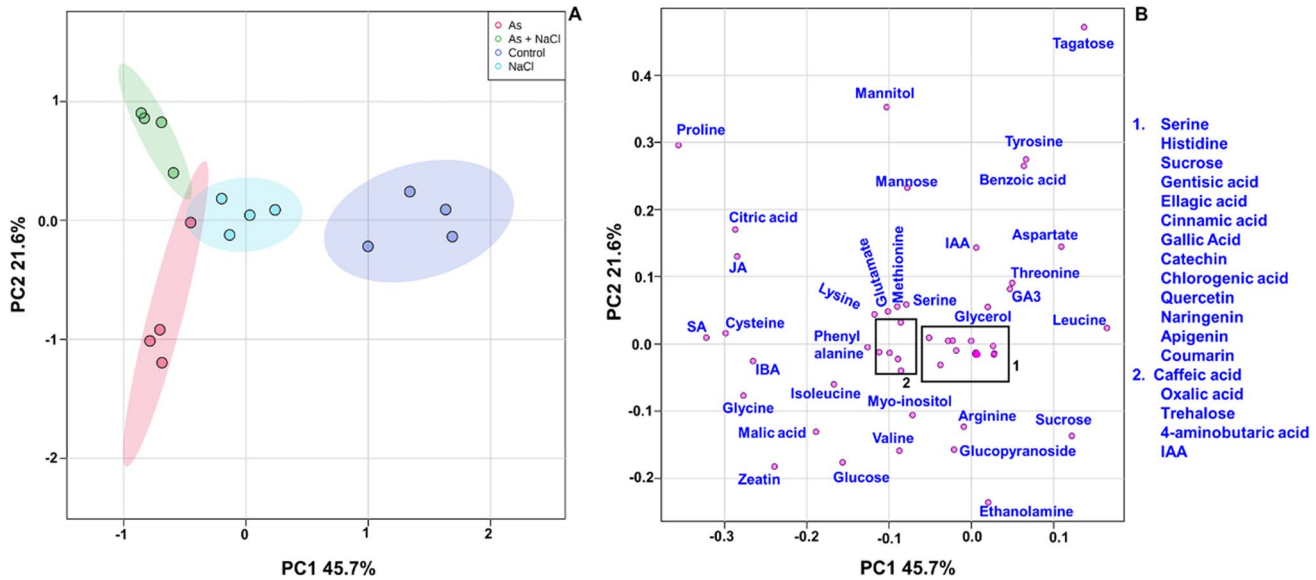

Fig. 4 Principal component analysis showing salinity- and arsenic-induced alterations in various metabolites in the root of *S. persica*. **A** Score plot. **B** Loading plot. PC1 and PC2 are the first and second principal components, respectively

be involved in mitigation of salt and/As stress including sugars, amino acids, organic acids, and phytohormones (Fig. 5). The metabolites such as tagatose, benzoic acid, isoleucine, aspartic acid, sucrose, and mannose showed noteworthy importance under high salinity. Moreover, IAA, mannose, sucrose, tagatose, histidine, ABA, aspartic acid, phenylalanine, glucose, glycine, proline, IBA, malic acid, and serine showed also noteworthy importance under

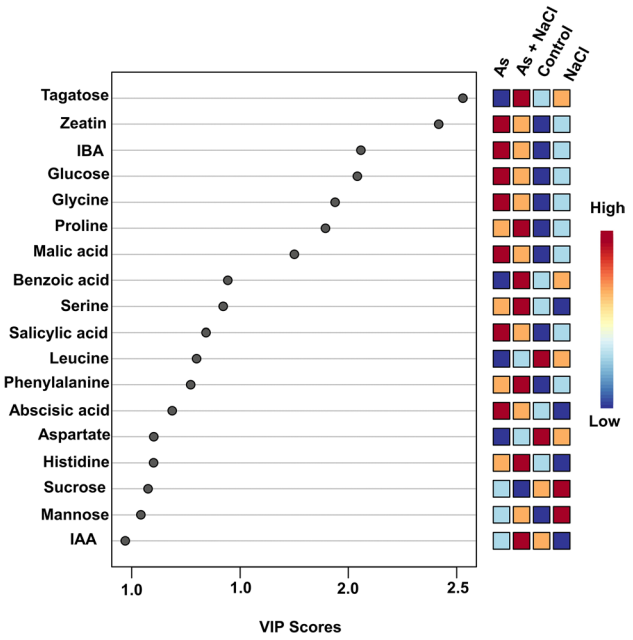

Fig. 5 VIP score plots demonstrating the most significantly changed metabolites in the root of *S. persica*

the solitary as well as combined effects of salinity and As (Fig. 5).

A Venn diagram was used to understand the responses of metabolites under stress conditions. In roots, a total of 25 metabolites were shared between control, high salinity, high As, and high As + 250 mM salinity (Fig. 6A, B). Moreover, 15 and 12 metabolites were differentially accumulated under high As and combined treatment of As + NaCl, respectively, of which 8 metabolites were specifically altered under high As, 5 metabolites were specifically altered under As + NaCl treatment, and 7 metabolites were shared between high As and As + NaCl (Fig. 6B). A total of seven metabolites which were significantly altered and commonly shared between the root of high As and combined treatment of As and salinity include lysine (0.7/1.3-fold), phenylalanine (1.2/1.3-fold), zeatin (2.3/1.2-fold), oxalic acid (0.38/0.36-fold), ethanolamine (0.6/-0.9-fold), lactic acid (-0.8/-1.1-fold), and sucrose (0.6/-1.5-fold) (Fig. 6B). Three metabolites such as serine ((-0.6/0.9-fold), mannose (1.4/1.2-fold), and naringenin (-0.48/0.6-fold) were commonly shared between high salinity and As + salinity (Fig. 6B). Eight metabolites which include arginine (0.5-fold), GA_3 (−0.7-fold), ABA (0.7-fold), benzoic acid (−1.7-fold), fructose (−1.4-fold), oxoproline (0.4-fold), scyllo-inositol (0.4-fold), and tagatose (−2.7-fold) were exclusively altered under high As stress.

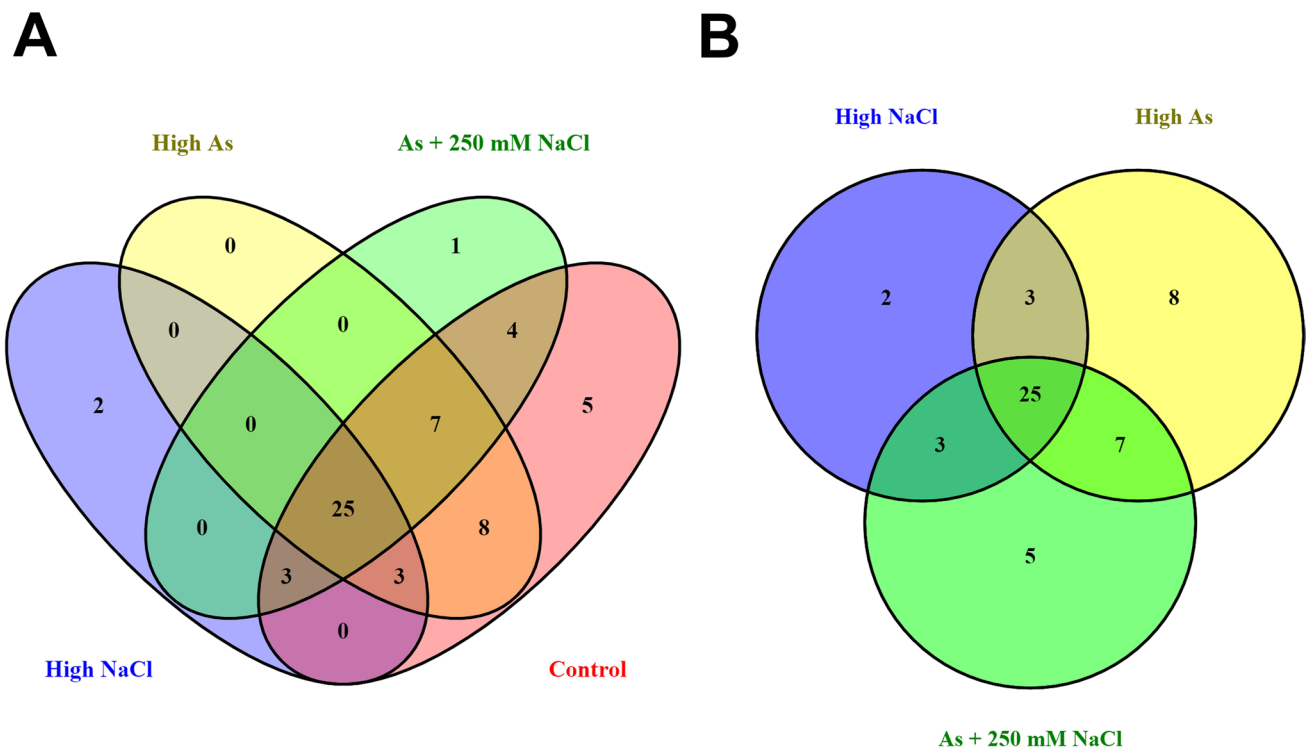

Fig. 6 Venn diagram analysis of salinity- and As-induced alterations in metabolites. **A** Distribution of metabolites. **B** Significantly altered metabolites among high NaCl, high As, and As + 250 mM NaCl treatments

Moreover, glucopyranose (1.5-fold) and sorbose (1.4-fold) were specifically altered under high salinity (Fig. 6B).

Salinity and/or As stress induced differential accumulations of metabolites in the root of *S. persica*

Among the identified metabolites, 15 were downregulated and 38 metabolites were upregulated under high salinity in *S. persica* (Fig. 7A). Our findings showed that most of the amino acids such as glutamate (+0.36-fold), glycine (+1.27-fold), alanine (+1.4-fold), proline (+1.57-fold), valine (+1.56-fold), cystine (+2.71-fold), isoleucine (+1.65-fold), phenylalanine (+0.43-fold), and lysine (+0.51-fold) were significantly upregulated under high salinity (Fig. 7A). However, serine (−0.62-fold), threonine (−1.2-fold), tyrosine (−1.3-fold), and leucine (−0.72-fold) content was significantly reduced in response to salinity. In addition, the concentration of various phytohormones like zeatin (+0.33-fold), IBA (+1.42-fold), JA (+threefold), and SA (+2.1-fold) remarkably increased, whereas IAA showed downregulation (−1.73-fold) under salinity. Among the organic acids and sugars, a remarkable increment was found in citric acid (+1.68-fold), malic acid (+0.58-fold), glucose (+0.44-fold), mannitol (+0.45-fold), mannose (+1.4-fold), sorbose (+1.44-fold), sucrose (+0.08-fold), galactose (+0.21-fold), scyllo-inositol (+0.27-fold), and myo-inositol (+0.66-fold). Furthermore, the levels of polyphenols such as caffeic acid (+0.77-fold), gentisic acid (+0.55-fold), ellagic acid (+0.2-fold), cinnamic acid (+0.58-fold), gallic acid (+0.91-fold), catechin (+0.5-fold), quercetin (+0.56-fold), apigenin (+0.68-fold), and coumarin (+0.55-fold) showed an increasing trend in response to salinity as compared to the control (Fig. 7A). Among the identified metabolites, the levels of 37 metabolites were increased and 18 metabolites were reduced under solitary As stress (Fig. 7B). In the case of combined stress of As + NaCl, 43 and 10 metabolites were upregulated and downregulated, respectively, as compared to control (Fig. 7C). Our data showed that the levels of glutamic acid (+0.79-fold), serine (+0.61-fold), glycine (+2.56-fold), histidine (+0.511-fold), proline (+2.16-fold), valine (+1.3-fold), cystine (+2.43-fold), isoleucine (+1.89-fold), phenylalanine (+1.21-fold), and lysine (+0.76-fold) increased remarkably under solitary treatment of As. The level of citrate (+1.47-fold), malate (+2.05-fold), oxalate (+0.38-fold), and glucose (+1.91-fold) was also significantly upregulated in response to solitary treatment of As. However, the levels of glutamic acid (+1.18-fold), serine (+0.98-fold), glycine (+2.36-fold), histidine (+1.05-fold), proline (+3.96-fold), cystine (+2.77-fold), phenylalanine (+1.32-fold), and lysine (+1.37-fold) were comparatively higher in the root of the plant treated with As supplemented with NaCl. Likewise, the concentration of IAA (+0.51-fold), ABA (+0.47-fold), IBA (+2.6-fold), SA (+2.46-fold), and JA (+3.26-fold) was significantly increased under As + NaCl compared to control. The concentration of citrate (+2.69-fold), mannose (+1.24-fold), mannitol (+1.99-fold), and galactose (+1.04-fold) also increased under combined As + NaCl stress. The polyphenols content also significantly enhanced under the combined treatment of As + NaCl. Our data showed enhanced accumulation of gallic acid (+0.92-fold), chlorogenic acid (+0.15-fold), quercetin (+1.05-fold), naringenin (+0.62-fold), apigenin (+0.49-fold), and coumarin (+0.93-fold) under combined stress of As + NaCl (Fig. 7C).

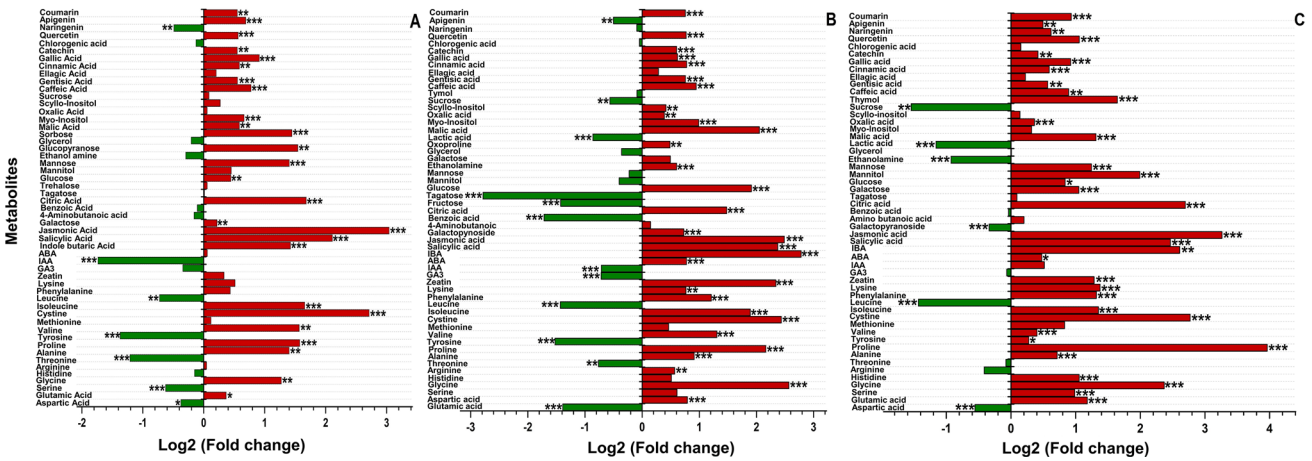

Fig. 7 Log_2 fold change variations of different metabolites in *S. persica* roots subjected to various levels of salinity and arsenic stress. **A** NaCl vs. control. **B** As vs. control. **C** As + NaCl vs. control. The positive and negative log_2 fold change values represent increased and decreased levels of metabolites, respectively. The asterisks "*", "**", and "***" demonstrate the statistically different metabolites at $P < 0.1$, $P < 0.05$, and $P < 0.01$, respectively

Correlation network and cluster analysis for elucidation of stress-related root metabolites

Both heatmap and correlation matrices are widely used in metabolomics studies to represent the level of metabolite expression and to clarify the relationships between identified metabolites under stress conditions. The heatmap analysis revealed that SA, trehalose, citric acid, cystine, JA, myo-inositol, mannitol, mannose, tagatose, and sucrose showed relatively higher abundance in response to salinity in comparison to control (Fig. 8). Furthermore, it is worth mentioning that the levels of organic acids (citric acid and benzoic acid), amino acids (tyrosine, threonine, glutamate, cystine, aspartic acid, histidine, and proline), sugars and sugar alcohols (mannose, tagatose, and mannitol), phytohormones (IAA, GA3, and JA) were comparatively higher, whereas the levels of malic acid, glycine, isoleucine, arginine, leucine, glucose, sucrose, myo-inositol, ABA, zeatin, and IBA were lower in combined treatment of As + NaCl as compared to solitary As treatment (Fig. 8). The data of the correlation matrix showed a strong positive correlation of root phytohormones (IBA, JA, zeatin, and SA) with mannose, glucose, sorbose, and myo-inositol. However, ABA and IAA were negatively correlated with these sugars under high saline conditions

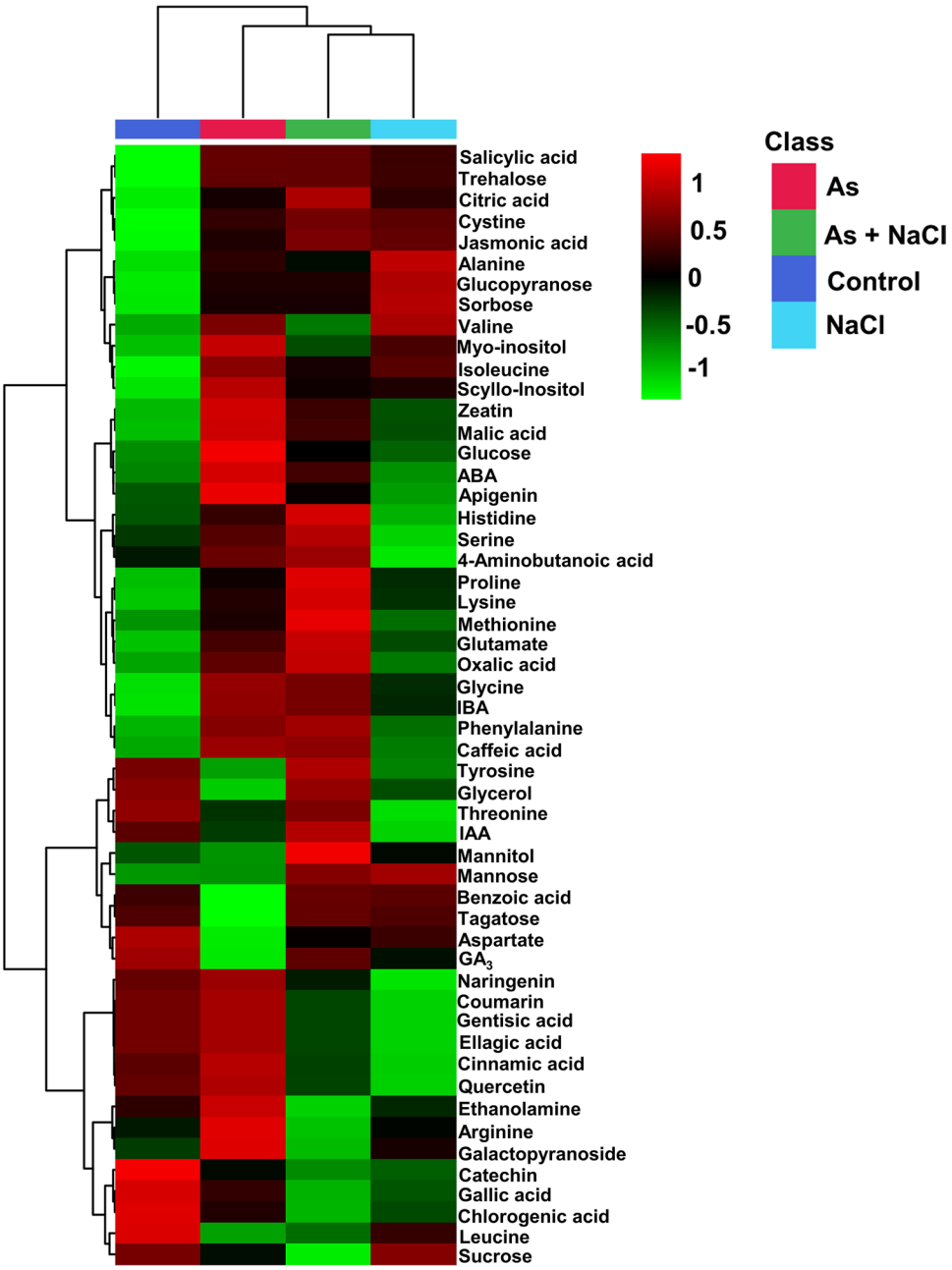

Fig. 8 Cluster analysis of NaCl- and As-induced alteration in root metabolites by heatmap

(Fig. 9A). It is worth mentioning that tyrosine exhibited a strong positive correlation with a group of polyphenols like ellagic acid, gentisic acid, naringenin, coumarin, chlorogenic acid, catechin, gallic acid, quercetin, and cinnamic acid (Fig. 9A). However, phenylalanine has a strong negative correlation with the above mentioned polyphenols. In addition, most of the amino acids were positively correlated with mannose, glucose, sorbose, and myo-inositol, and showed negative correlation with sucrose, tagatose, glycerol, and trehalose (Fig. 9A). Glucose was positively correlated with ABA under As with and without salt. Glycine, cystine, and glutamate were positively correlated with each other (Fig. 9B and C). The levels of metal-chelating amino acids (histidine, cysteine, and proline) strongly correlated with organic acids (oxalate, malate, and citrate). Moreover, salicylic acid showed strong positive correlation with ABA and auxins, and negative correlation with GA_3 under As + salinity stress. However, in the case of solitary As, salicylic acid was strongly negatively correlated with GA_3 and auxins, and showed strong positive correlation with ABA.

Metabolic pathways analysis in root treated with salinity and/As stress

Using *Arabidopsis thaliana* KEGG pathway library, a pathway enrichment analysis was performed to analyze salinity and As-induced alterations in various metabolic pathways. The pathway enrichment analysis results specified 23 metabolic pathways, which remarkably affected by NaCl and/or As conditions (Fig. 10). High salinity significantly altered alanine, aspartate, and glutamate metabolism, glycine, serine, and threonine metabolism, isoquinoline alkaloid biosynthesis, tyrosine metabolism, phenylalanine metabolism, glyoxylate and dicarboxylate metabolism, arginine and proline metabolism, glutathione metabolism, cysteine and methionine metabolism, citrate cycle, ascorbate and aldarate metabolism, inositol phosphate metabolism, and tryptophan metabolism having pathway impact and pathway enrichment [-log10(p)] values are > 0.1 and > 0.5, respectively (Fig. 10A and Table 1). The pathways that significantly changed under As stress were ascorbate and aldarate metabolism, glyoxylate and dicarboxylate metabolism, glutathione metabolism, TCA cycle, glycine, serine and threonine metabolism, inositol phosphate metabolism cysteine and methionine metabolism, alanine, aspartate, and glutamate metabolism, isoquinoline alkaloid biosynthesis, tyrosine metabolism, arginine biosynthesis, arginine and proline metabolism, butanoate metabolism, tryptophan metabolism, and phenylpropanoid biosynthesis having pathway impact and pathway enrichment values > 0.1 and > 1, respectively (Fig. 10B, and Table 2). The pathways that changed significantly under arsenic + salinity treatment were alanine, aspartate and glutamate metabolism, arginine biosynthesis, cystine and methionine metabolism, stilbenoid, diarylheptanoid, and gingerol biosynthesis, glutathione metabolism glyoxylate and dicarboxylate metabolism, citrate cycle, arginine and proline metabolism, glycine, serine, and threonine metabolism, ascorbate and aldarate metabolism, flavonoid biosynthesis, and phenylalanine metabolism having pathway impact and pathway enrichment [-log10(p)] values > 0.1 and > 1, respectively (Fig. 10C and Table 3). The schematic representation of the alterations of different root metabolites and metabolic pathways is depicted in Fig. 11.

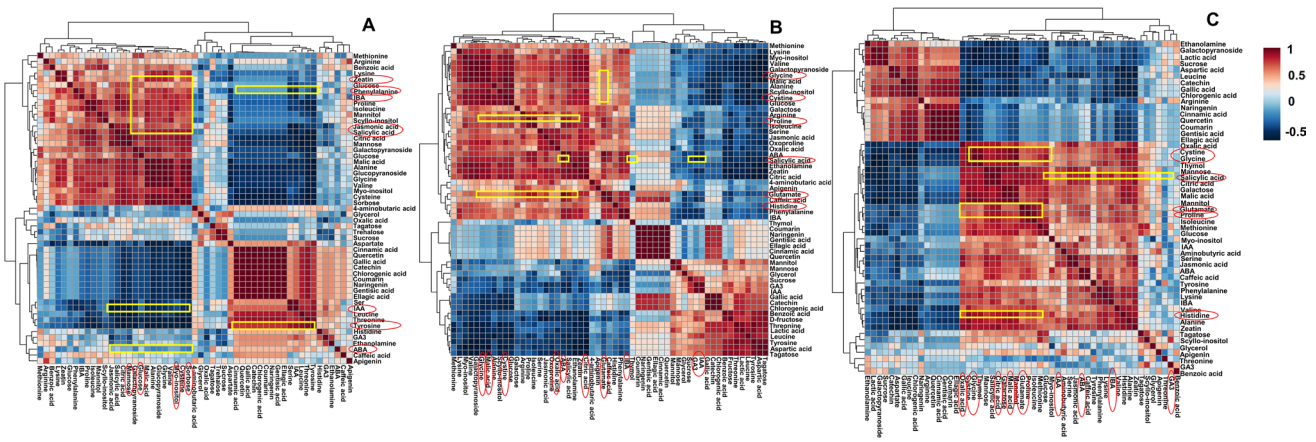

Fig. 9 Cluster analysis of NaCl- and As-induced alteration in root metabolites by correlation matrix. **A** 750 mM NaCl. **B** 600 µM As. **C** 600 µM As + 250 mM NaCl

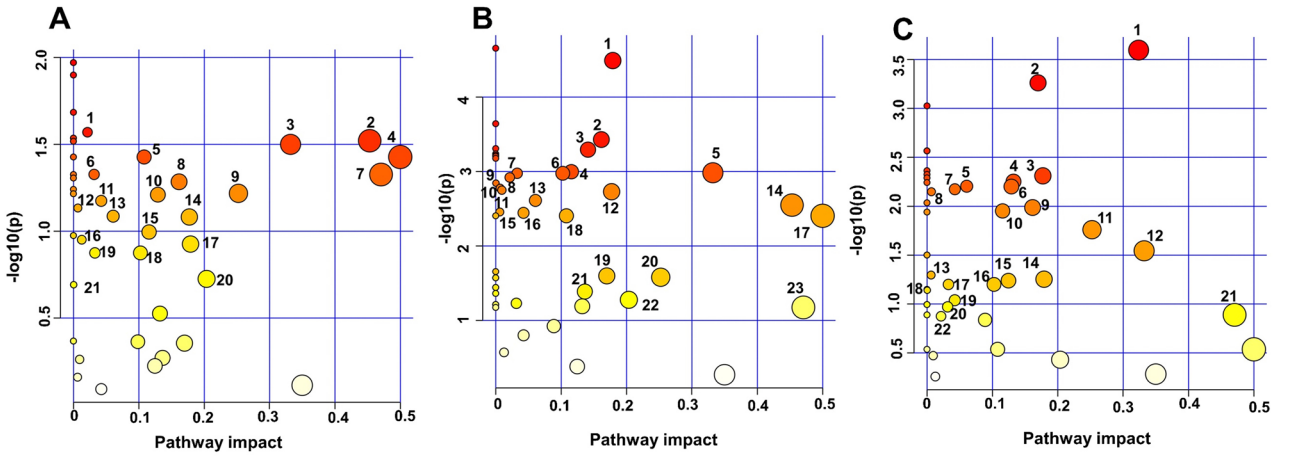

1. Phenylalanine, tyrosine and tryptophan biosynthesis
2. Alanine, aspartate and glutamate metabolism
3. Glycine, serine and threonine metabolism
4. Isoquinoline alkaloid biosynthesis
5. Tyrosine metabolism
6. Phenylpropanoid biosynthesis
7. Phenylalanine metabolism
8. Glyoxylate and dicarboxylate metabolism
9. Arginine and proline metabolism
10. Glutathione metabolism
11. Galactose metabolism
12. Zeatin biosynthesis
13. Sulfur metabolism
14. Cysteine and methionine metabolism
15. Citrate cycle (TCA cycle)
16. Glycerolipid metabolism
17. Ascorbate and aldarate metabolism
18. Inositol phosphate metabolism
19. Phosphatidylinositol signaling system
20. Tryptophan metabolism
21. Glycolysis / Gluconeogenesis

1. Ascorbate and aldarate metabolism
2. Glyoxylate and dicarboxylate metabolism
3. Glutathione metabolism
4. Citrate cycle (TCA cycle)
5. Glycine, serine and threonine metabolism
6. Inositol phosphate metabolism
7. Phosphatidylinositol signaling system
8. Phenylalanine, tyrosine and tryptophan biosynthesis
9. Glycolysis / Gluconeogenesis
10. Zeatin biosynthesis
11. Glycerophospholipid metabolism
12. Cysteine and methionine metabolism
13. Sulfur metabolism
14. Alanine, aspartate and glutamate metabolism
15. Carotenoid biosynthesis
16. Galactose metabolism
17. Isoquinoline alkaloid biosynthesis
18. Tyrosine metabolism
19. Arginine biosynthesis
20. Arginine and proline metabolism
21. Butanoate metabolism
22. Tryptophan metabolism
23. Phenylpropanoid biosynthesis

1. Alanine, aspartate and glutamate metabolism
2. Arginine biosynthesis
3. Cysteine and methionine metabolism
4. Stilbenoid, diarylheptanoid and gingerol biosynthesis
5. Sulfur metabolism
6. Glutathione metabolism
7. Histidine metabolism
8. Zeatin biosynthesis
9. Glyoxylate and dicarboxylate metabolism
10. Citrate cycle (TCA cycle)
11. Arginine and proline metabolism
12. Glycine, serine and threonine metabolism
13. Carotenoid biosynthesis
14. Ascorbate and aldarate metabolism
15. Flavonoid biosynthesis
16. Inositol phosphate metabolism
17. Phosphatidylinositol signaling system
18. Glycolysis / Gluconeogenesis
19. Galactose metabolism
20. Phenylpropanoid biosynthesis
21. Phenylalanine metabolism
22. Phenylalanine, tyrosine and tryptophan biosynthesis

Fig. 10 Graphical representation of pathway enrichment analysis showing the metabolome view of and changes in different metabolic pathways in response to various treatments. **A** Salinity (750 mM NaCl). **B** Arsenic (600 µM As). **C** Arsenic + salinity (600 µM As + 250 mM NaCl)

Discussion

A low level of salinity helps to diminish As-induced ROS in *S. persica*

The excessive production of reactive oxygen species (ROS) is one of the prime responses of the plants toward salinity and arsenic stress, which are involved in oxidative damages to the cellular components (Ahmad et al. 2010). ROS are persistently generated in plants as surplus products in the chloroplasts, peroxisomes, apoplasts, plasma membrane, and mitochondria during various metabolic pathways. Overproduction of ROS reduced the membrane fluidity, thus increased electron leakage, damage membrane proteins, and inactivate receptors and enzymes (Nabi et al. 2021). In the current investigation, high salt and As treatment significantly accumulated MDA content. In consistence with our results, increased MDA level has been recorded in maize roots under heavy metals (Zn, Cu, and Cd) stress (AbdElgawad et al. 2020). Likewise, the increased MDA content has also been observed in *Cakile maritima* root exposed to high salinity (Houmani et al. 2022). In the current study, both NaCl and As increased the level of $O_2^{\bullet-}$ and H_2O_2 in the root. Whereas, the level of ROS was significantly reduced when low salinity was applied with As stress. The accumulation of H_2O_2 in plant tissues confers the heavy metal tolerance of plants by stimulating the antioxidant system (Cuypers et al. 2016). Furthermore, the accumulation

Table 1 Pathway analysis of altered metabolic pathways in the root of *S. persica* under salinity stress

Pathway	Total Cmpd	Hits	Raw P	Log(P)	Holm adjust	FDR	Impact
Glucosinolate biosynthesis	65	5	0.0107	1.9706	0.48152	0.13215	0
Valine, leucine and isoleucine degradation	37	3	0.01262	1.8989	0.55529	0.13215	0
Valine, leucine and isoleucine biosynthesis	22	4	0.02069	1.6842	0.88967	0.13215	0
Phenylalanine, tyrosine and tryptophan biosynthesis	22	2	0.026942	1.5696	1	0.13215	0.02152
Selenocompound metabolism	13	1	0.029114	1.5359	1	0.13215	0
Carbon fixation in photosynthetic organisms	21	1	0.029114	1.5359	1	0.13215	0
Alanine, aspartate, and glutamate metabolism	22	3	0.030155	1.5206	1	0.13215	0.45324
Aminoacyl-tRNA biosynthesis	46	15	0.030372	1.5175	1	0.13215	0
Glycine, serine, and threonine metabolism	33	2	0.031647	1.4997	1	0.13215	0.33218
Isoquinoline alkaloid biosynthesis	6	1	0.037402	1.4271	1	0.13215	0.5
Tyrosine metabolism	16	1	0.037402	1.4271	1	0.13215	0.10811
Ubiquinone and other terpenoid-quinone biosynthesis	38	1	0.037402	1.4271	1	0.13215	0
Phenylpropanoid biosynthesis	46	2	0.047126	1.3267	1	0.13215	0.03161
Phenylalanine metabolism	11	1	0.047191	1.3261	1	0.13215	0.47059
Tropane, piperidine, and pyridine alkaloid biosynthesis	8	1	0.047191	1.3261	1	0.13215	0
Pantothenate and CoA biosynthesis	23	2	0.049445	1.3059	1	0.13215	0
Glyoxylate and dicarboxylate metabolism	29	4	0.051961	1.2843	1	0.13215	0.16159
Cyanoamino acid metabolism	29	3	0.057482	1.2405	1	0.13215	0
Arginine and proline metabolism	34	4	0.060584	1.2176	1	0.13215	0.25242
Thiamine metabolism	22	2	0.060909	1.2153	1	0.13215	0
Glutathione metabolism	26	3	0.061669	1.2099	1	0.13215	0.12915
Galactose metabolism	27	3	0.066925	1.1744	1	0.13689	0.04252
Zeatin biosynthesis	21	1	0.073573	1.1333	1	0.14395	0.00678
Sulfur metabolism	15	1	0.082023	1.0861	1	0.14926	0.06077
Cysteine and methionine metabolism	46	2	0.082921	1.0813	1	0.14926	0.17729
Citrate cycle (TCA cycle)	20	1	0.10116	0.99497	1	0.17034	0.11571
Lysine biosynthesis	9	1	0.10599	0.97473	1	0.17034	0
Lysine degradation	18	1	0.10599	0.97473	1	0.17034	0
Glycerolipid metabolism	21	1	0.11208	0.95046	1	0.17392	0.01277
Ascorbate and aldarate metabolism	18	2	0.11872	0.92549	1	0.17807	0.1791
Inositol phosphate metabolism	28	1	0.13347	0.87461	1	0.1877	0.10251
Phosphatidylinositol signaling system	26	1	0.13347	0.87461	1	0.1877	0.03285
Tryptophan metabolism	28	1	0.18841	0.72491	1	0.25692	0.2037
Glycolysis / gluconeogenesis	26	1	0.20357	0.69129	1	0.26943	0.00038
Stilbenoid, diarylheptanoid, and gingerol biosynthesis	8	1	0.29841	0.52519	1	0.38366	0.13235
Porphyrin and chlorophyll metabolism	48	1	0.42949	0.36704	1	0.50975	0
Nitrogen metabolism	12	1	0.42949	0.36704	1	0.50975	0
Starch and sucrose metabolism	22	2	0.43334	0.36318	1	0.50975	0.09857
Arginine biosynthesis	18	2	0.44178	0.35479	1	0.50975	0.16991
Butanoate metabolism	17	2	0.53699	0.27003	1	0.60128	0.13636
Glycerophospholipid metabolism	37	1	0.54783	0.26135	1	0.60128	0.00947
Flavonoid biosynthesis	47	4	0.59729	0.22382	1	0.63995	0.12466
Carotenoid biosynthesis	43	1	0.6933	0.15908	1	0.72555	0.00632
Flavone and flavonol biosynthesis	10	2	0.77184	0.11247	1	0.78938	0.35
Histidine metabolism	15	1	0.8123	0.090285	1	0.8123	0.04264

of H_2O_2 in the root could also be considered a protective mechanism under heavy metal stress. It has been reported that increased H_2O_2 induced the lignification of the root cell wall, thereby restricting the heavy metal translocation (Schützendübel et al. 2001; Cuypers et al. 2002). In corroboration with our result, increased H_2O_2 content has been

Table 2 Pathway analysis of altered metabolic pathways in the root of *S. persica* under arsenic stress

Pathway	Total Cmpd	Hits	Raw P	Log10(P)	Holm adjust	FDR	Impact
Aminoacyl-tRNA biosynthesis	46	15	2.21E-05	4.6565	0.001037	0.000759	0
Ascorbate and aldarate metabolism	18	2	3.23E-05	4.4909	0.001486	0.000759	0.1791
Glucosinolate biosynthesis	65	5	0.000228	3.6427	0.010245	0.003124	0
Glyoxylate and dicarboxylate metabolism	29	4	0.000372	3.4299	0.016351	0.003124	0.16159
Valine, leucine, and isoleucine degradation	37	3	0.000491	3.3087	0.021122	0.003124	0
Glutathione metabolism	26	4	0.000508	3.2942	0.021332	0.003124	0.14117
Cyanoamino acid metabolism	29	3	0.000578	3.2382	0.023689	0.003124	0
Valine, leucine, and isoleucine biosynthesis	22	4	0.000605	3.2184	0.024193	0.003124	0
Pantothenate and CoA biosynthesis	23	2	0.000626	3.2037	0.0244	0.003124	0
Thiamine metabolism	22	2	0.000665	3.1774	0.025254	0.003124	0
Citrate cycle (TCA cycle)	20	1	0.001005	2.9977	0.037197	0.003542	0.11571
Glycine, serine, and threonine metabolism	33	2	0.001038	2.9838	0.037368	0.003542	0.33218
Inositol phosphate metabolism	28	1	0.001055	2.9767	0.037368	0.003542	0.10251
Phosphatidylinositol signaling system	26	1	0.001055	2.9767	0.037368	0.003542	0.03285
Phenylalanine, tyrosine, and tryptophan biosynthesis	22	2	0.001199	2.9211	0.039572	0.003757	0.02152
Glycolysis / gluconeogenesis	26	2	0.001432	2.8441	0.045818	0.004206	0.00038
Zeatin biosynthesis	21	1	0.001672	2.7769	0.051817	0.004617	0.00678
Glycerophospholipid metabolism	37	1	0.001779	2.7499	0.053365	0.004617	0.00947
Cysteine and methionine metabolism	46	2	0.001866	2.729	0.054122	0.004617	0.17729
Sulfur metabolism	15	1	0.002445	2.6117	0.068456	0.005745	0.06077
Alanine, aspartate, and glutamate metabolism	22	3	0.002825	2.549	0.076263	0.006322	0.45324
Carotenoid biosynthesis	43	1	0.003496	2.4565	0.09089	0.007109	0.00632
Galactose metabolism	27	4	0.003592	2.4447	0.09089	0.007109	0.04252
Isoquinoline alkaloid biosynthesis	6	1	0.003933	2.4053	0.094385	0.007109	0.5
Tyrosine metabolism	16	1	0.003933	2.4053	0.094385	0.007109	0.10811
Ubiquinone and other terpenoid-quinone biosynthesis	38	1	0.003933	2.4053	0.094385	0.007109	0
Amino sugar and nucleotide sugar metabolism	50	1	0.022099	1.6556	0.46407	0.038468	0
Arginine biosynthesis	18	2	0.025256	1.5976	0.50513	0.040619	0.16991
Arginine and proline metabolism	34	4	0.026326	1.5796	0.50513	0.040619	0.25242
Selenocompound metabolism	13	1	0.026791	1.572	0.50513	0.040619	0
Carbon fixation in photosynthetic organisms	21	1	0.026791	1.572	0.50513	0.040619	0
Porphyrin and chlorophyll metabolism	48	1	0.036113	1.4423	0.5778	0.051433	0
Nitrogen metabolism	12	1	0.036113	1.4423	0.5778	0.051433	0
Butanoate metabolism	17	2	0.040992	1.3873	0.5778	0.056666	0.13636
Pyruvate metabolism	22	1	0.04344	1.3621	0.5778	0.058334	0
Tryptophan metabolism	28	1	0.052905	1.2765	0.63486	0.06907	0.2037
Phenylpropanoid biosynthesis	46	2	0.059	1.2291	0.649	0.073756	0.03161
Lysine biosynthesis	9	1	0.061202	1.2132	0.649	0.073756	0
Lysine degradation	18	1	0.061202	1.2132	0.649	0.073756	0
Stilbenoid, diarylheptanoid, and gingerol biosynthesis	8	1	0.06469	1.1892	0.649	0.074942	0.13235
Phenylalanine metabolism	11	1	0.06697	1.1741	0.649	0.074942	0.47059
Tropane, piperidine, and pyridine alkaloid biosynthesis	8	1	0.06697	1.1741	0.649	0.074942	0
Starch and sucrose metabolism	22	1	0.11932	0.92328	0.649	0.13042	0.0889
Histidine metabolism	15	1	0.15882	0.7991	0.649	0.16964	0.04264
Glycerolipid metabolism	21	1	0.26912	0.57005	0.80737	0.28108	0.01277
Flavonoid biosynthesis	47	4	0.41655	0.38033	0.8331	0.42561	0.12466
Flavone and flavonol biosynthesis	10	2	0.53719	0.26987	0.8331	0.53719	0.35

Table 3 Pathway analysis of altered metabolic pathways in the root of *S. persica* under NaCl + As stress

Pathway	Total Cmpd	Hits	Raw P	Log10(P)	Holm adjust	FDR	Impact
Alanine, aspartate, and glutamate metabolism	22	2	0.000253	3.5961	0.01166	0.01166	0.32374
Arginine biosynthesis	18	2	0.000548	3.2613	0.024653	0.0126	0.16991
Aminoacyl-tRNA biosynthesis	46	15	0.000942	3.0259	0.041452	0.014445	0
Butanoate metabolism	17	1	0.002716	2.5661	0.11678	0.020433	0
Porphyrin and chlorophyll metabolism	48	1	0.002716	2.5661	0.11678	0.020433	0
Nitrogen metabolism	12	1	0.002716	2.5661	0.11678	0.020433	0
Valine, leucine, and isoleucine degradation	37	3	0.00433	2.3635	0.17321	0.020433	0
Valine, leucine, and isoleucine biosynthesis	22	4	0.004726	2.3255	0.18432	0.020433	0
Cysteine and methionine metabolism	46	2	0.004888	2.3109	0.18574	0.020433	0.17729
Glucosinolate biosynthesis	65	5	0.005127	2.2901	0.1897	0.020433	0
Stilbenoid, diarylheptanoid, and gingerol biosynthesis	8	1	0.00559	2.2526	0.20125	0.020433	0.13235
Pantothenate and CoA biosynthesis	23	2	0.00572	2.2426	0.20125	0.020433	0
Sulfur metabolism	15	1	0.006243	2.2046	0.21228	0.020433	0.06077
Glutathione metabolism	26	3	0.006288	2.2015	0.21228	0.020433	0.12915
Histidine metabolism	15	1	0.006701	2.1739	0.21442	0.020433	0.04264
Zeatin biosynthesis	21	1	0.007107	2.1483	0.22032	0.020433	0.00678
Thiamine metabolism	22	2	0.00922	2.0353	0.2766	0.024949	0
Glyoxylate and dicarboxylate metabolism	29	4	0.010308	1.9868	0.29892	0.026342	0.16159
Citrate cycle (TCA cycle)	20	1	0.011165	1.9521	0.31262	0.026366	0.11571
Cyanoamino acid metabolism	29	3	0.011463	1.9407	0.31262	0.026366	0
Arginine and proline metabolism	34	3	0.017365	1.7603	0.45149	0.038038	0.25242
Glycine, serine and threonine metabolism	33	2	0.02855	1.5444	0.71375	0.059696	0.33218
Selenocompound metabolism	13	1	0.031538	1.5012	0.75692	0.060449	0
Carbon fixation in photosynthetic organisms	21	1	0.031538	1.5012	0.75692	0.060449	0
Carotenoid biosynthesis	43	1	0.050548	1.2963	1	0.093008	0.00632
Ascorbate and aldarate metabolism	18	2	0.055742	1.2538	1	0.09822	0.1791
Flavonoid biosynthesis	47	4	0.057651	1.2392	1	0.09822	0.12466
Inositol phosphate metabolism	28	1	0.063006	1.2006	1	0.09994	0.10251
Phosphatidylinositol signaling system	26	1	0.063006	1.2006	1	0.09994	0.03285
Pyruvate metabolism	22	1	0.070731	1.1504	1	0.10717	0
Glycolysis / gluconeogenesis	26	2	0.07222	1.1413	1	0.10717	0.00038
Galactose metabolism	27	4	0.091371	1.0392	1	0.13135	0.04252
Lysine biosynthesis	9	1	0.10118	0.99491	1	0.13689	0
Lysine degradation	18	1	0.10118	0.99491	1	0.13689	0
Phenylpropanoid biosynthesis	46	2	0.10684	0.97126	1	0.14042	0.03161
Phenylalanine metabolism	11	1	0.129	0.88941	1	0.16038	0.47059
Tropane, piperidine, and pyridine alkaloid biosynthesis	8	1	0.129	0.88941	1	0.16038	0
Phenylalanine, tyrosine, and tryptophan biosynthesis	22	2	0.13329	0.87521	1	0.16135	0.02152
Starch and sucrose metabolism	22	1	0.14512	0.83827	1	0.17117	0.0889
Isoquinoline alkaloid biosynthesis	6	1	0.2901	0.53745	1	0.31773	0.5
Tyrosine metabolism	16	1	0.2901	0.53745	1	0.31773	0.10811
Ubiquinone and other terpenoid-quinone biosynthesis	38	1	0.2901	0.53745	1	0.31773	0
Glycerophospholipid metabolism	37	1	0.33676	0.47268	1	0.36025	0.00947
Tryptophan metabolism	28	1	0.3704	0.43132	1	0.38724	0.2037
Flavone and flavonol biosynthesis	10	2	0.52003	0.28397	1	0.53159	0.35
Glycerolipid metabolism	21	1	0.55073	0.25906	1	0.55073	0.01277

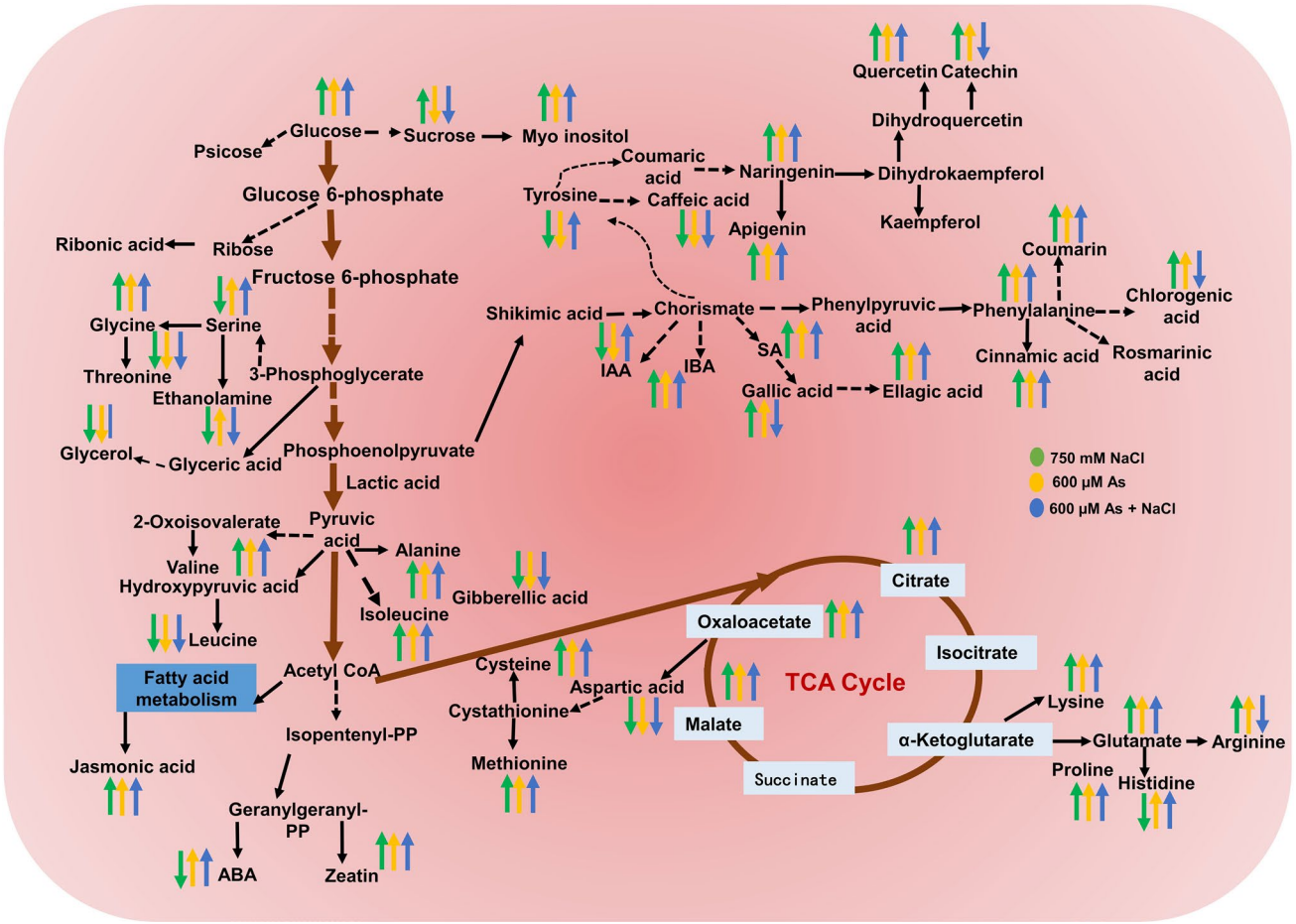

Fig. 11 Pathway overview displaying the differentially altered metabolites in *S. persica* roots exposed to salinity and arsenic stress. The upward arrow (↑), downward arrow (↓), and vertical lines (|) represent upregulation, downregulation, and no significant changes, respectively

reported in soybean roots under heavy metals stress (Bilal et al. 2019). The increase in MDA and H_2O_2 concentration upon salt stress has also been reported in *Crithmum maritimum* root (Hamed et al. 2007).

Alteration in the levels of antioxidants efficiently eliminates salinity and As-generated ROS and maintains redox homeostasis in the cell

Plants have the potential to develop a robust antioxidative defensive mechanism to scavenge excess harmful radicals. They upregulate the antioxidative system to avoid oxidative damage to macromolecules and cellular structures under stress conditions. Plants use different enzymatic antioxidant components like SOD, CAT, APX, GR, and GPX and non-enzymatic antioxidants like proline, AsA, and GSH to recover from the deleterious consequences of oxidative stress. In the present study, the activity of SOD, CAT, GPX, and GR significantly increased under As stress. However, the level of APX was significantly reduced under high As and remained unchanged in response to high salinity. SOD scavenges excessive amount of $O_2^{\bullet-}$ radicals and plays an essential role in ROS homeostasis and reduces damage induced by heavy metal stress. SOD scavenges $O_2^{\bullet-}$ radicals by converting them into H_2O_2 and O_2. The generated H_2O_2 can be further decomposed by APX, CAT, GR, and GPX or catalyzed by the ascorbate–glutathione pathway into water and oxygen. GR and APX play crucial roles in the AsA-GSH cycle and are responsible for the cellular control of H_2O_2. Moreover, higher expression of GR suggests the regeneration of GSH that could have been directly oxidized by ROS (Gill et al. 2013). Our results showed the higher activity of SOD, CAT, GPX, and GR under salinity and/or As stress in roots of *S. persica*. The activity of APX and GPX has been reported to be elevated in the roots of the halophyte *Sesuvium portulacastrum* upon salt stress (Kulkarni et al. 2022). Similar to our findings, higher expression of SOD, CAT, guaiacol peroxidase (POX), and APX has also been demonstrated in maize roots treated with heavy metals (AbdElgawad et al. 2020). Furthermore, the elevated levels of SOD and H_2O_2

have been reported in *Kandelia obovata* root tissues under cadmium stress (Pan et al. 2019).

The non-enzymatic antioxidants work in a coordinated fashion with enzymatic antioxidants to inhibit the excess production of ROS. The glutathione is the most abundant water-soluble low-molecular-weight thiol in the plants. It plays a crucial role in sequestering heavy metals and metalloids, protecting the cellular components against ROS (Ghori et al. 2019). The ratio of reduced to oxidized glutathione maintains the redox buffer of the cells and upholds the reduced environment in the cell. The glutathione mainly counters heavy metal stress by controlling the level of H_2O_2, and during the detoxification of H_2O_2, glutathione is oxidized. The ratio of GSH:GSSG is often used as a marker of ROS production and redox homeostasis in the cells. During oxidative stress, the reduced form of glutathione (GSH) can directly scavenge free radicals and tightly regulate ROS homeostasis. GSH is a derivative of cysteine, glycine, and glutamic acid and acts as a ligand to chelate heavy metals and reduce their toxicity. GSH is also involved in reducing As(V) to As(III), which can bind to the –SH group of the phytochelatin (PCs). PCs have a strong affinity toward heavy metals and form a stable bond with metals and translocate in the vacuole medium, thus decrease the free metals concentration in the plant cell (Yu et al. 2019). In the current investigation, the GSH level increased with a concomitant decrease in GSSG content under salinity and/or As conditions. The higher glutathione redox ratio in the root under As and combined stress of As + NaCl suggests the induction of As-stress-induced oxidative stress tolerance mechanism by *S. persica*. In contrast to our study, AbdElgawad et al. (2020) have documented declined GSH/GSSG ratio in maize roots under heavy metal stress. Our results indicate that high GSH in the root might be involved in the phytochelatins synthesis, hence higher chelation of As in the root of *S. persica*.

Phytohormone cross-talk mitigates oxidative stress and plays an imperative role in stress tolerance

In plants, hormone concentration and regulation are closely linked to the environment, oxidative stress, plant nutrient uptake, and metabolism (Zemanová et al. 2019). The upregulation of hormone biosynthesis and signaling genes suggests their role in stress management. Phytohormones cross-talk triggers the signaling pathways in a very specific and controlled way, eliciting defense against adverse environments. Plants induce the higher accumulation of growth regulators like auxin (IAA), ABA, JA, and SA under environmental stimuli. Plant growth regulators have synergistic or antagonistic interactions in different tissues, developmental stages, and environmental conditions. ABA is a multifaceted phytohormone that controls different physio-biochemical processes in plants. The concentration of ABA increases in response to heavy metal stress attributed to its role in the induction of protective mechanisms in plants against toxic metals. It has been reported that the genes *PHT1;1* and *NIPs* are responsible for the uptake and distribution of As whose expression can be downregulated by ABA. Thus, ABA reduced As distribution and detoxification by activation of *MYB-NIPs* (Hu et al. 2020). Our results showed that As and/or salinity significantly increased the concentration of ABA in the root of *S. persica*, whereas the ABA level was decreased in response to high salinity. In agreement with our result, ABA concentration remarkably reduced under high salinity and remained at par with the control level when a low level of salt was applied with Cd in the root of *S. portulacastrum* (Wali et al. 2016). The increase in ABA has also been reported in *Kandelia obovata* root tissue under cadmium stress (Pan et al. 2020). Cd treatment induces the synthesis of ABA in roots of *T. latifolia*, *P. australis* (Fediuc et al. 2005), and potato tubers (Stroinski et al. 2010).

Jasmonic acid plays an important role in plant stress signaling under adverse environments. GSH accumulation is essential to upregulate the JA signaling pathway. Furthermore, JA alleviates heavy metal toxicity by stimulating the signal transduction cascade, ROS homeostasis, and activating stress-responsive genes. Our data showed that the amount of JA and SA was significantly enhanced by NaCl and/or As stress. It has been reported that JA alleviates As-induced oxidative stress by modulating the AsA-GSH cycle in oilseed rape roots (Farooq et al. 2018). Furthermore, a constant level of JA has been reported in response to high salinity and combined treatment of low salinity with Cd in the root of *S. portulacastrum* (Wali et al. 2016). Salicylic acid (SA) maintains membrane integrity by stimulating the antioxidant defense system under salinity (Jayakannan and Bose 2015). SA plays a major role in the induction of antioxidant potential and enhances GSH and GSH:GSSG levels to cope the environmental stresses (Ghanta et al. 2014). SA also cross-talks with other phytohormones such as auxin, GA_3, and ABA and stimulates the antioxidant enzymes, detoxifies ROS, maintains membrane integrity, and increases the efficiency of the photosystem. It has been reported that Cd treatment increases the accumulation of SA in the root of *S. portulacastrum,* whereas it is reduced when low level of salt is applied with Cd (Wali et al. 2016). The levels of IAA, ABA, zeatin, and GA_3 show an upward trend in *A. thaliana* root in response to heavy metal stress (Vitti et al. 2014). Auxin (IAA and IBA) is a dynamic mediator in plants controlling many developmental stages under both stress and non-stressful conditions. In plants, an optimum IAA level is essential for the development and establishment of root system. The role of auxin has been reported in the induction of various biological processes and activation of antioxidant (both enzymatic and non-enzymatic) systems in response to metalloid stress in the plant (Singh

et al. 2021). In the present report, the amount of auxin significantly improved under combined treatment of As and salt than only As suggests the role of auxin in As stress tolerance in this halophyte.

Upraised root osmolytes maintain osmotic homeostasis under salinity and/or arsenic stress condition

The plants counteract the stressful environment through internal osmotic adjustment by accumulating osmotically active compounds known as osmolytes/compatible solutes. The osmolytes are non-toxic, and highly soluble organic solutes that encompass sugars, sugar alcohols, amino acids, amines, and betaines. Under stressful conditions, these compounds guard the cells by maintaining the water uptake, membrane structure, stabilizing cellular protein, maintaining redox balance, scavenging free radicals, and helping the plants to activate its antioxidative defense mechanism. Therefore, it is obvious that these compounds also protect the cellular structures and enzyme molecules from salinity and heavy metal toxicity. Further, the ability of the halophytes to rapidly synthesize these osmolytes under ion toxicity may be explained by their ability to detoxify the metal (loid)s toxicity (Lutts and Lefever 2015). The plant cells actively synthesize some osmotic solutes such as soluble sugars and amino acids to reduce intracellular osmotic potential, to maintain water supply for normal physiological functions in plants under heavy metal stress conditions (Yu et al. 2019). Sugars and hormones are crucial for remote signaling in plants. Glucose and sucrose play essential roles in auxin biosynthesis and are involved in ABA signaling (Gangola and Ramadoss 2018). Our data showed that the levels of glucose, galactose, and myo-inositol were elevated under both As and NaCl stress. The concentration of various sugars like fructose, tagatose, mannitol, mannose, and sucrose was significantly reduced in response to As stress. However, the levels of these sugars were enhanced by the addition of salt even in the presence of high As in *S. persica* roots. The increased concentration of sugars in the root indicates its role in osmotic adjustment and stress signaling to combat As stress in *S. persica*. The concentrations of glucose and fructose remain constant and galactose level significantly increases in the root of *Populus nigra* under heavy metal stress (Stobrawa and Lorenc-Plucińska 2007). The accumulation of glucose, talose, threonine, myo-inositol, and galactinol has also been reported in the root of *Sesuvium portulacastrum* exposed to salinity stress (Kulkarni et al. 2022).

Amino acids are important metabolites that play crucial roles in maintenance of osmotic balance, stress signaling, nutrient absorption, and heavy metal(loid)s chelation (Fu et al. 2018). It has been reported that secretion of the amino acids in the plant root is enhanced significantly when exposed to heavy metal stress (Fu et al. 2019). In the current investigation, the concentrations of glycine, alanine, proline, valine, cysteine, isoleucine, and lysine were significantly increased, whereas the pool of aspartic acid, serine, threonine, tyrosine, and leucine was significantly decreased in response to high salinity. It should be worth mentioning that the level of glutamic acid, serine, histidine, proline, lysine, methionine, cysteine, and phenylalanine showed higher accumulation under the combined stress of salt and As than solitary As in the root. The enrichment analysis revealed that alanine, aspartate, and glutamate metabolism, glycine, serine, and threonine metabolism, arginine and proline metabolism, phenylalanine metabolism, cysteine, and methionine metabolism were top-rank pathways under salinity and/or As stress (Tables 1, 2, 3). The increased amino acids pool maintains hydration within the cell and protects the cell from severe oxidative injury during As stress (Ahmad et al. 2020). The concentrations of methionine, lysine, and histidine are increased in the root of rice under the Cd stress (Wang et al. 2016). The levels of threonine, alanine, serine, GABA, and oxo-proline also upregulate in the root of *Sesuvium portulacastrum* exposed to salinity stress (Kulkarni et al. 2022). The concentrations of lysine, arginine, histidine alanine, valine, leucine, isoleucine, and methionine are enhanced in *Kandelia obovata* root under Cd stress (Xie et al. 2013). The important role of proline has also been reported as a metal chelator, ROS scavenger, and signaling molecule, thus overcoming oxidative stress (Mansour and Ali 2017). Histidine playing a critical role in heavy metal chelation and transportation is considered as an important free amino acid in heavy metal metabolism. Various functional groups (carboxylic group, pyridinic nitrogen, amino group, and pyrrolic nitrogen site) present in histidine are used to chelate heavy metals (Wang et al. 2016). The methionine metabolism pathway effectively scavenged peroxide production due to oxidative stress in response to heavy metal stimuli (She et al. 2015). The increased concentration of glutamic acid, glycine, and cysteine in root of *S. persica* suggests their involvement in the synthesis of thiol-rich peptides such as GHS and phytochelatin for efficient detoxification of As in the root of *S. persica*. This hypothesis was further confirmed by the pathway enrichment results indicating the glutathione metabolism was top-rank pathway under As with and without salinity stress.

Accumulations of phenolic compounds and organic acids play crucial roles in As chelation and sequestration in roots, thus reducing As toxicity in *S. persica*

The plants activate various mechanisms to reduce and counteract the deleterious impacts of heavy metals (loid)s. Plant

phenolics are a group of secondary metabolites synthesized via the shikimic acid/phenylpropanoid pathway. The phenolic compounds are efficient antioxidants that can scavenge free radicals and chelate metal (loid)s. Phenolic compounds act as non-enzymatic antioxidants that activate and strengthen plant defense mechanisms. The metal chelation activity of phenols is directly associated with the molecule's high nucleophilic character of the aromatic rings (Khanna et al. 2019). Polyphenols are not only involved in metal chelation but can also reduce ROS toxicity by the Fenton reaction. Phenolic compounds also inhibit lipid peroxidation by capturing lipid alkoxyl radicals generated during the stress (Chauhan et al. 2017). The differential regulations of phenolics explain their defensive role in plants against adverse environments. Phenolic acids such as caffeic, cinnamylmalic, gallic, ferulic, and vanillic acids have strong antioxidant potential and enhance the plant tolerance to abiotic stress (Samec et al. 2021). In the present study, the levels of caffeic acid, gentisic acid, ellagic acid, cinnamic acid, gallic acid, catechin, and coumarin significantly increased under both solitary and combined treatment of salinity and As. However, supplemented salt improved the accumulation of phenolics compound under As stress in *S. persica*. The phenylpropanoid biosynthesis and flavonoid biosynthesis pathways were significantly altered under NaCl and/or As (Tables 1, 2, 3). Coumaric acid polymerization results in cell wall lignification, which is correlated to metal stress resistance (Samec et al. 2021). Gallic acid with ellagic acid protects the plants from heavy metal toxicity by chelation of metals and metalloids (Samec et al. 2021). Naringenin has a high antioxidant efficiency to decompose free radicals like hydroxyl and superoxide. Arsenic stress increases the content of ferulic acid and rutin, and decreases gallic acid, chlorogenic acid, protocatechuic acid, and caffeic acid in the roots of rice (Chauhan et al. 2017). The higher phenolics pool in the root of *S. persica* suggests their important role in free radical detoxification and As chelation.

Organic acids are important metabolites in plants mainly involved in the TCA cycle and glyoxylate cycle. Low-molecular-weight organic acids like citrate, oxalate, malate, and tartrate are secreted in large amount by metal hyperaccumulator plants, which are often associated with metal stress tolerance by long-distance transport of metals through the xylem and accumulation in the vacuole (Fu et al. 2018). Organic acids form a strong bond with metal ions by one or more carboxylic groups and chelate heavy metals, thereby reducing their toxicity. Citric acid synthesized by citrate synthase has a comparatively higher affinity to chelate metal ions than malic acid and oxalic acid in plants. In the current investigation, the concentrations of citrate, malate, and oxalate were significantly increased by both high NaCl and As stress. However, the citrate content was further elevated when a low level of salt was supplied with high As. Moreover, the citrate cycle was a top-rank pathway under both solitary and combine treatment of salinity and As (Tables 1, 2, 3). The accumulated organic acids may help As to reach the vascular region of the root in *S. persica.* In agreement with our result, the accumulation of citrate cycle (TCA cycle) metabolites such as oxalic acid, malic acid, citrate, tartarate, and acetate has been reported in roots of *Kandelia obovata* and rice (Xie et al. 2013; Fu et al. 2018). The increased levels of TCA cycle components including succinate, malate, and citrate have also been reported in the root of the halophyte *Sesuvium portulacastrum* exposed to salinity stress (Kulkarni et al. 2022).

Conclusion

Overall, our results demonstrated that *S. persica* (xero-halophyte) is well adapted to thrive under high NaCl and As conditions. The coordinative action of both, non-enzymatic and enzymatic antioxidants, efficiently mitigates oxidative stress, regulates ROS level, and protects the membrane integrity during stress condition. Our study highlights that the halophyte *S. persica* can stabilize maximum As in the root by inducing the synthesis of phytochelatins and safely sequestering it in the root vacuoles by the formation of As-PCs complex, thereby protecting the photosynthetic system. Higher level of ABA, JA, SA, and auxin elicits the antioxidative defense system and reduces ROS and As toxicity in the root system. The elevation of some important amino acids like glycine, histidine, cysteine, proline, and glutamate is attributed to their function in ROS scavenging, regulation of osmotic homeostasis, and synthesis of metal chelators like PCs and glutathione under As and salinity stress. The higher accumulation of various sugars such as glucose, sucrose, galactose, mannitol, and mannose provides osmotic adjustment, energy, antioxidative defense, carbon skeleton for secondary metabolite synthesis, and efficient signaling to achieve salinity and As stress tolerance. The accumulated organic acid could efficiently chelate As, thereby ameliorating As toxicity in the plant. The enhanced phenylalanine metabolism leads to a higher synthesis of many polyphenolic compounds (quercetin, naringenin, apigenin, coumarin, gallic acid, and catechin) that maintains ROS at threshold level and provides salinity and As tolerance to *S. persica*. A schematic model demonstrating As tolerance mechanisms and the alleviatory role of NaCl in detoxification of As in the root of *S. persica* has been shown in Fig. 12. The pathway enrichment analysis identified pathways correlated to amino acid metabolism, glutathione metabolism, sugar metabolism, TCA cycle, phenylpropanoid biosynthesis, phenylalanine metabolism, and inositol phosphate metabolism which are involved in As tolerance. The modulations in these pathways, their

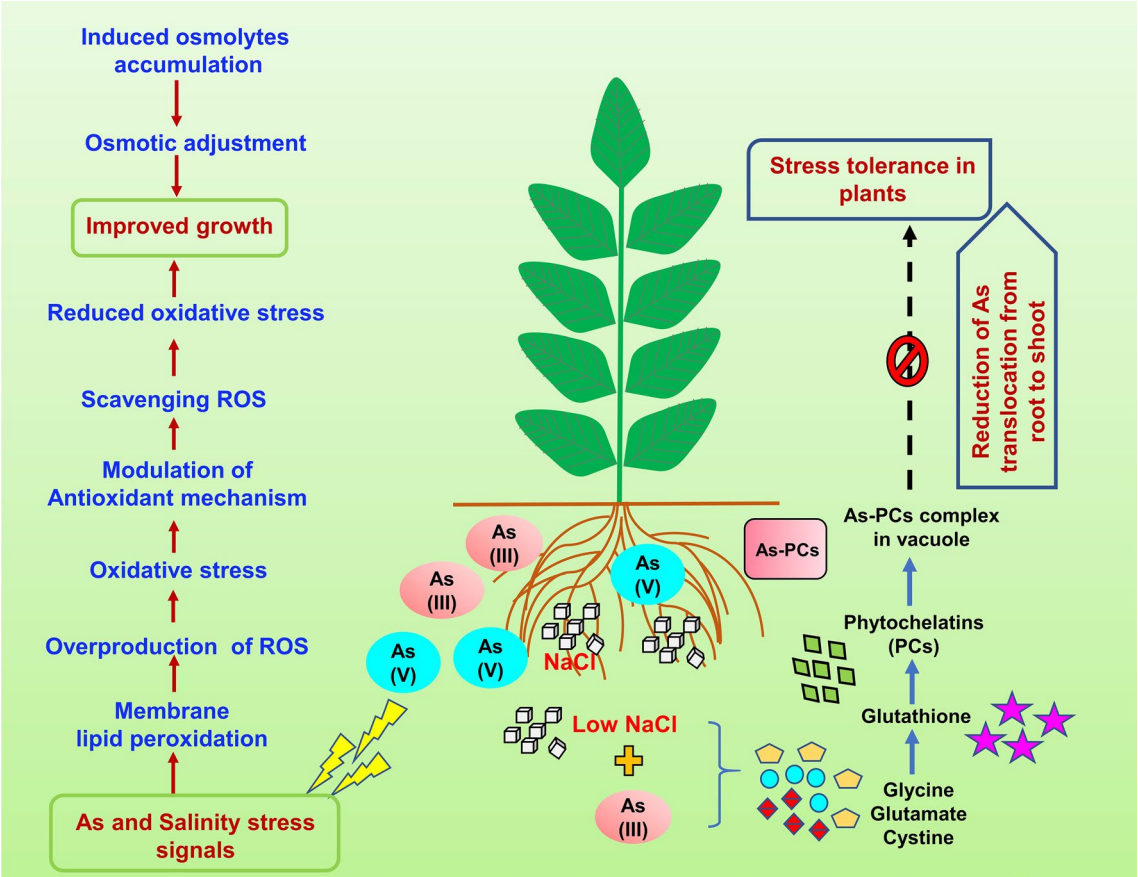

Fig. 12 A schematic model showing As tolerance mechanisms and influence of salinity on As detoxification in *S. persica*

intermediates, and products provide a framework to resist high salinity and arsenic. The presented results will expand our understanding of NaCl and As cross-tolerance and the potential use of *S. persica* in the phytoremediation of As contamination. The information generated from this study can be employed for the development of salinity and As resistant crops using transgenic approach.

Acknowledgements The financial support from the Department of Science and Technology (DST) by the grant of SERB (SERB/SB/SO/PS-14/2014), DST, Government of India, New Delhi to AKP is duly acknowledged. This work was also supported by the fund from the Department of Science & Technology, Government of India, New Delhi, in the form of Inspire Fellowship (DST/Inspire Fellowship/2016/IF160267) to MP. This manuscript bears CSIR-CSMCRI registration number 154/2023.

Author contributions MP carried out the experiments, data acquisition, analyzed the data, and prepared manuscript. AKP conceptualized, designed and coordinated the experiments, interpreted the results, and improved manuscript.

Data availability statement All the data generated or analyzed during this study are included in this article.

Declarations

Conflict of interest The authors declare that they have no conflict of interest.

References

AbdElgawad H, Zinta G, Hamed BA et al (2020) Maize roots and shoots show distinct profiles of oxidative stress and antioxidant defense under heavy metal toxicity. Environ Poll 258:113705

Ahmad P, Jaleel CA, Salem MA et al (2010) Roles of enzymatic and nonenzymatic antioxidants in plants during abiotic stress. Crit Rev Biotechnol 30:161–175

Ahmad P, Alam P, Balawi TH et al (2020) Sodium nitroprusside (SNP) improves tolerance to arsenic (As) toxicity in *Vicia faba* through the modifications of biochemical attributes, antioxidants, ascorbate-glutathione cycle and glyoxalase cycle. Chemosphere 244:125480

Bilal S, Shahzad R, Khan AL (2019) Phytohormones enabled endophytic *Penicillium funiculosum* LHL06 protects *Glycine max* L. from synergistic toxicity of heavy metals by hormonal and stress-responsive proteins modulation. J Hazar Mater 379:120824

Bradford MM (1976) A rapid and sensitive method for the quantitation of microgram quantities of protein utilizing the principle of protein-dye binding. Anal Biochem 72:248–254

Chauhan R, Awasthi S, Tripathi P (2017) Selenite modulates the level of phenolics and nutrient elements to alleviate the toxicity of arsenite in rice (*Oryza sativa* L.). Ecotoxicol Environ Saf 138:47–55

Cuypers ANN, Vangronsveld J, Clijsters H (2002) Peroxidases in roots and primary leave of *Phaseolus vulgaris* copper and zinc phytotoxicity: a comparison. J Plant Physiol 159:869–876

Cuypers A, Hendrix S, Amaral dos RR et al (2016) Hydrogen peroxide, signaling in disguise during metal phytotoxicity. Front Plant Sci 7:470

Farooq MA, Islam F, Yang C et al (2018) Methyl jasmonate alleviates arsenic-induced oxidative damage and modulates the ascorbate-glutathione cycle in oilseed rape roots. Plant Growth Regul 84:135–148

Fediuc E, Lips SH, Erdei L (2005) O-acetylserine (thiol) lyase activity in *Phragmites* and *Typha* plants under cadmium and NaCl stress conditions and the involvement of ABA in the stress response. J Plant Physiol 23:865–872

Fu H, Yu H, Li T, Zhang X (2018) Influence of cadmium stress on root exudates of high cadmium accumulating rice line (*Oryza sativa* L.). Ecotoxicol Environ Saf 150:168–175

Gangola MP, Ramadoss BR (2018) Sugars play a critical role in abiotic stress tolerance in plants. In: Wani SH (Ed) Biochemical, physiological and molecular avenues for combating abiotic stress in plants. Elsevier Inc./Academic Press, pp17–38

Ghanta S, Datta R, Bhattacharyya D et al (2014) Multistep involvement of glutathione with salicylic acid and ethylene to combat environmental stress. J Plant Physiol 171:940–950

Ghori NH, Ghori T, Hayat MQ et al (2019) Heavy metal stress and responses in plants. Int J Environ Sci Technol 16:1807–1828

Gill SS, Anjum NA, Hasanuzzaman M et al (2013) Glutathione and glutathione reductase: a boon in disguise for plant abiotic stress defense operations. Plant Physiol Biochem 70:204–212

Hamed BK, Castagna A, Salem E, Ranieri A, Abdelly C (2007) Sea fennel (Crithmum maritimum L.) under salinity conditions: a comparison of leaf and root antioxidant responses. Plant Growth Regul 53:185–194

Houmani H, Palma JM, Corpas FJ (2022) High salinity stimulates the adaptive response to potassium deficiency through the antioxidant and the NADPH-generating systems in the roots and leaves of the halophyte Cakile maritima. J Plant Growth Regul 42:6286–6306

Hu B, Deng F, Chen G et al (2020) Evolution of abscisic acid signaling for stress responses to toxic metals and metalloids. Front Plant Sci 11:909

Ibáñez H, Ballester A, Muñoz R, Quiles JM (2010) Chlororespiration and tolerance to drought, heat and high illumination. J Plant Physiol 167:732–738

Jamla M, Khare T, Joshi S, Patil S et al (2021) Omics approaches for understanding heavy metal responses and tolerance in plants. Curr Plant Biol 27:100213

Jayakannan M, Bose J (2015) Salicylic acid in plant salinity stress signalling and tolerance. Plant Growth Regul 76:25–40

Khanna K, Lakshmi V, Sharma A, Gandhi SG et al (2019) Supplementation with plant growth promoting rhizobacteria (PGPR) alleviates cadmium toxicity in *Solanum lycopersicum* by modulating the expression of secondary metabolites. Chemosphere 230:628–639

Kulkarni J, Sharma S, Sahoo SA, Mishra S (2022) Resilience in primary metabolism contributes to salt stress adaptation in *Sesuvium portulacastrum* (L.). Plant Growth Regul 98:385–398

Kumari A, Parida AK (2018) Metabolomics and network analysis reveal the potential metabolites and biological pathways involved in salinity tolerance of the halophyte *Salvadora persica*. Environ Exp Bot 148:85–99

Kwanyuen P, Burton JW (2010) A modified amino acid analysis using PITC derivatization for soybeans with accurate determination of cysteine and half-cystine. JAOCS, J Am Oil Chem Soc 87:127–132

Liu JJ, Diao ZH, Xu XR, Xie Q (2019) Effects of dissolved oxygen, salinity, nitrogen and phosphorus on the release of heavy metals from coastal sediments. Sci Total Environ 666:894–901

Lutts S, Lefever I (2015) How can we take advantage of halophyte properties to cope with heavy metal toxicity in salt-affected areas? Ann Bot 115:509–528

Mansour MMF, Ali EF (2017) Evaluation of proline functions in saline conditions. Phytochemistry 140:52–68

Martínez-Castillo JI, Saldana-Robles A, Ozuna C (2022) Arsenic stress in plants: a metabolomic perspective. Plant Stress 3:100055

Nabi A, Naeem M, Aftab T, Khan MMA et al (2021) A comprehensive review of adaptations in plants under arsenic toxicity: physiological, metabolic and molecular interventions. Environ Pollut 290:118029

Nikalje GC, Suprasanna P (2018) Coping with metal toxicity-cues from halophytes. Front Plant Sci 9:777

Pan X, Welti R, Wang X (2010) Quantitative analysis of major plant hormones in crude plant extracts by high-performance liquid chromatography-mass spectrometry. Nat Protoc 5:986–992

Pan C, Lu H, Yu J et al (2019) Identification of Cadmium-responsive Kandelia obovata SOD family genes and response to Cd toxicity. Environ Exp Bot162:230–238

Pan C, Lu H, Liu J, Yu J (2020) SODs involved in the hormone mediated regulation of H_2O_2 content in *Kandelia obovata* root tissues under cadmium stress. Environ Pol 256:113272

Parida AK, Jha B (2010) Antioxidative defense potential to salinity in the euhalophyte *Salicornia brachiata*. J Plant Growth Regul 29:137–148

Patel M, Parida AK (2021) Salinity alleviates the arsenic toxicity in the facultative halophyte *Salvadora persica* L. by the modulations of physiological, biochemical, and ROS scavenging attributes. J Hazard Mater 401:123368

Patel M, Parida AK (2022) Salinity mediated cross-tolerance of arsenic toxicity in the halophyte *Salvadora persica* L. through metabolomic dynamics and regulation of stomatal movement and photosynthesis. Environ Pol 300:118888

Patel MK, Pandey S, Tanna B, Alkam N, Mishra M (2022) Comparative metabolomics unveils the role of metabolites and metabolic pathways in the adaptive mechanisms of shrubby halophytes. Environ Exp Bot 202:105030

Phulwaria M, Ram K, Gahlot P, Shekhawat NS (2011) Micropropagation of *Salvadora persica* - a tree of arid horticulture and forestry. New Forest 42:317–327

Rahman SU, Xuebin Q, Kamran M (2021) Silicon elevated cadmium tolerance in wheat (*Triticum aestivum* L.) by endorsing nutrients uptake and antioxidative defense mechanisms in the leaves. Plant Physiol Biochem 166:148–159

Rahman SU, Nawaz MF, Gul S et al (2022) State-of-the-art OMICS strategies against toxic effects of heavy metals in plants: A review. Ecotoxico Environ Saf 242:113952

Rai PK, Sonne C, Kim KH (2023) Heavy metals and arsenic stress in food crops: Elucidating antioxidative defense mechanisms in hyperaccumulators for food security, agricultural sustainability, and human health. Sci Total Environ 874:162327

Rangani J, Parida AK, Panda A, Kumari A (2016) Coordinated changes in anti-oxidative enzymes protect the photosynthetic machinery from salinity induced oxidative damage and confer salt tolerance in an extreme halophyte *Salvadora persica* L. Front Plant Sci 7:50

Rangani J, Panda A, Patel M, Parida AK (2018) Regulation of ROS through proficient modulations of antioxidative defense system maintains the structural and functional integrity of photosynthetic apparatus and confers drought tolerance in the facultative

halophyte *Salvadora persica* L. J Photochem Photobiol B Biol 189:214–233
Rangani J, Panda A, Kumar A (2020) Metabolomic study reveals key metabolic adjustments in the xerohalophyte *Salvadora persica* L. during adaptation to water deficit and subsequent recovery conditions. Plant Physiol Biochem 150:180–195
Reddy MP, Shah MT, Patolia JS (2008) *Salvadora persica*, a potential species for industrial oil production in semiarid saline and alkali soils. Ind Crops Prod 8:273–278
Roessner U, Lytovchenko A, Carrari F (2003) Metabolic profiling of transgenic tomato plants overexpressing hexokinase reveals that the influence of hexose phosphorylation diminishes during fruit development. Plant Physiol 133:84–99
Samec D, Karalija E, Sola I, Vuj V (2021) The role of polyphenols in abiotic stress response: the influence of molecular structure. Plants 10:118
Sarath NG, Shackira AM, El-Serehy HA, Hefft DI, Puthur JT (2022) Phytostabilization of arsenic and associated physio-anatomical changes in *Acanthus ilicifolius* L. Environ Pol 298:118828
Schützendübel A, Schwanz P, Teichmann T et al (2001) Cadmium-induced changes in antioxidative systems, hydrogen peroxide content, and differentiation in scots pine roots. Plant Physiol 127:887–898
She W, Zhu S, Jie Y et al (2015) Expression profiling of cadmium response genes in ramie (*Boehmeria nivea* L.) root. Bull Environ Contam Toxicol 94:453–459
Singh H, Bhat JA, Singh VP (2021) Auxin metabolic network regulates the plant response to metalloids stress. J Hazar Mater 405:124250
Stobrawa K, Lorenc-Plucińska G (2007) Changes in carbohydrate metabolism in fine roots of the native European black poplar (*Populus nigra* L.) in a heavy-metal-polluted environment. Sci Total Environ 373:157–165
Stroinski A, Chadzinikolau T, Gizewska K, Zielezinska M (2010) ABA or cadmium induced phytochelatin synthesis in potato tubers. Biol Plant 54:117–120
Vitti A, Nuzzaci M, Scopa A (2014) Hormonal response and root architecture in *Arabidopsis thaliana* subjected to heavy metals. Int J Plant Biol 5:5226
Vromman D, Martínez JP, Kumar M et al (2018) Comparative effects of arsenite (As (III)) and arsenate (As(V)) on whole plants and cell lines of the arsenic-resistant halophyte plant species *Atriplex atacamensis*. Environ Sci Pollut Res 25:34473–34486
Wali M, Gunsè B, Llugany M et al (2016) High salinity helps the halophyte *Sesuvium portulacastrum* in defense against Cd toxicity by maintaining redox balance and photosynthesis. Planta 244:333–346
Wang Q, Chen L, He LY, Sheng XF (2016) Increased biomass and reduced heavy metal accumulation of edible tissues of vegetable crops in the presence of plant growth-promoting *Neorhizobium huautlense* T1–17 and biochar. Agric Ecosyst Environ 228:9–18
Xie X, Weiss DJ, Weng B et al (2013) The short-term effect of cadmium on low molecular weight organic acid and amino acid exudation from mangrove (*Kandelia obovata* (S L.) Yong) roots. Environ Sci Pollut Res 20:997–1008
Yang H, Wu F, Cheng J (2011) Reduced chilling injury in cucumber by nitric oxide and the antioxidant response. Food Chem 127:1237–1242
Yu G, Ma J, Jiang P et al (2019) The mechanism of plant resistance to heavy metal. In: IOP Conf. Series: Earth Environ Science 310: 052004
Zemanová V, Pavlíková D, Dobrev PI et al (2019) Endogenous phytohormone profiles in *Pteris* fern species differing in arsenic accumulating ability. Environ Exp Biol 166:103822
Zhang J, Yang D, Li M, Shi L (2016) Metabolic profiles reveal changes in wild and cultivated soybean seedling leaves under salt stress. PLoS ONE 11:e0159622